

# Minimal criteria for continuous-variable genuine multipartite entanglement

Olga Leskovjanová and Ladislav Mišta, Jr.

Department of Optics, Palacký University, 17. listopadu 12, 771 46 Olomouc, Czech Republic

We derive a set of genuine multi-mode entanglement criteria for second moments of the quadrature operators. The criteria have a common form of the uncertainty relation between sums of variances of position and momentum quadrature combinations. A unique feature of the criteria is that the sums contain the least possible number of variances of at most two-mode combinations. The number of second moments we need to know to apply the criteria thus scales only linearly with the number of modes, as opposed to the quadratic scaling of the already existing criteria. Each criterion is associated with a tree graph, which allowed us to develop a direct method of construction of the criteria based solely on the structure of the underlying tree. The practicality of the proposed criteria is demonstrated by finding a number of examples of Gaussian states of up to six modes, whose genuine multi-mode entanglement is detected by them. The designed criteria are particularly suitable for verification of genuine multipartite entanglement in large multi-mode states or when only a set of two-mode nearest-neighbour marginal covariance matrices of the investigated state is available.

## 1 Introduction

At the very foundations of the quantum information theory lies the effort to explain possible relationships between a pair of quantum systems. These relationships manifest itself through various forms of correlations which we try to capture by intuitive models complying better with our idea of how the nature ought to work. Then we can classify states of a composite system into a nested family of sets according to whether the state admits a separable model [1, 2], local hidden state model [3, 4] or local hidden variable model [5, 6]. The absence of the model then points at a closer relationship between the subsystems, which is referred to as entanglement, steering and non-locality, and which can be used as a resource for quantum communication and computing [7].

Olga Leskovjanová: [ola.leskovjanova@gmail.com](mailto:ola.leskovjanova@gmail.com)

Ladislav Mišta, Jr.: [mista@optics.upol.cz](mailto:mista@optics.upol.cz)

The complexity of the relationships is significantly increased in systems consisting of three or more subsystems, called commonly as the multipartite systems. From the point of view of quantum entanglement, states of multipartite systems can be classified into two disjoint sets. One is the set of so-called biseparable states, which can be prepared by statistical mixing of states that are separable with respect to (generally different) partitions of all subsystems into two groups. The second is then the set of states that cannot be prepared in this way, which we refer to as genuine multipartite entangled (GME) [8].

Genuine multiparticle entanglement is of great importance both in terms of fundamental research and applications. The GME carried by the Greenberger-Horne-Zeilinger (GHZ) state exhibits a strong contradiction with locally realistic theories, which can be captured without the use of the Bell-type statistical inequalities [9, 10]. The same state also serves as an ideal testbed for the analysis of the scaling law of the coherence decay of a multiparticle quantum register [11]. Early applications of GME included quantum secret sharing protocol [12] or assisted quantum teleportation schemes [13, 14]. In newer applications, GME is used to increase the precision of phase estimation in interferometry [15, 16] and it also plays a key role in the measurement-based model of quantum computing [17, 18], in which the computation is performed using a sequence of local single-site measurements on a large GME state. Last but not least, GME is also a resource for multiparty quantum key distribution [19, 20].

Motivated by both the fundamental questions of many-body physics and the desire to demonstrate the advantage of quantum computers compared to classic ones, experimenters have been trying to create ever-larger GME states. An important part of characterizing these states is obviously the ability to detect the GME. There are at least three reasons for this. First, certification of GME confirms the presence of a key resource for measurement-based model of quantum computing [17]. Second, detection of the GME is crucial for understanding of the entanglement dynamics in a simulated system [21]. Finally, on a general level successful generation of GME evidences a high degree of control which was gained over the used experimental platform [22].

Attempts to prepare a large GME state are

proceeding in two directions. One uses systems with a two-dimensional Hilbert state space (qubits), while the other relies on systems with an infinite-dimensional Hilbert state space, the so-called continuous-variable (CV) systems. Nowadays, preparation of the qubit GME states is limited to the medium-scale systems. This includes preparation of the 14 ion qubits in the GHZ state [11], 18-qubit photonic GHZ state [23] or 51-qubit cluster state on a superconducting quantum processor [24] to name at least few of them.

A more auspicious framework for preparation of a large GME state is provided by Gaussian states of CV systems [25]. These systems are realized typically by optical modes and they are characterized by canonically conjugate position  $x$  and momentum  $p$  quadrature operators. Gaussian states possess a Gaussian-shaped Wigner function and they are easily prepared, manipulated and measured in the laboratory. Additionally, entanglement properties of an  $N$ -mode Gaussian state are completely characterized by  $N(2N + 1)$  independent elements of its covariance matrix and thus the number of parameters determining the state grows quadratically with the number of modes. Although so far only three-mode [26, 27] and four-mode [28, 29] Gaussian GME states have been demonstrated in the laboratory, medium-scale to large-scale Gaussian states possessing a weaker form of global entanglement, known as the full inseparability, have been already observed experimentally. Specifically, a fully inseparable 10-mode [28] and 60-mode [30] state has been prepared using optical frequency comb, and 10 000-mode [31] or even one-million-mode [32] fully inseparable state has been generated by means of the time-domain multiplexing.

There are two basic ways in which the CV GME can be detected. The first one utilizes the GME witness in the space of covariance matrices [33]. It requires knowledge of the entire covariance matrix, or its entire position and momentum part, and so far it has been used exclusively for verification of the GME in the theoretical states [34, 35]. The second approach is based on simpler CV GME criteria [26, 29, 36, 37], which are more transparent and more economical in terms of the number of needed measurements. All the criteria are built on the van Loock-Furusawa criterion of full inseparability [38], which generalizes Duan's *et al.* criterion of two-mode entanglement [39] and its bipartite generalization [40] to the multi-mode case. The considered criteria are usually designed to detect in a simple way some paradigmatic GME Gaussian states and therefore they are of the form of a single inequality for the second moments of the quadrature operators. As an example can serve us the sum version of the criterion [26], according to which a three-

mode state is GME if the inequality

$$\begin{aligned} \langle [\Delta(x_1 - x_2)]^2 \rangle + \langle [\Delta(x_2 - x_3)]^2 \rangle \\ + \langle [\Delta(p_1 + p_2 + p_3)]^2 \rangle \geq 2 \end{aligned} \quad (1)$$

is violated. The criterion exhibits a common feature of the overwhelming majority of the practically used GME criteria. Namely, some (more often all [27, 36]) occurring variances contain a global combination of all position or momentum quadratures. For the three-mode criterion (1) the combination in question is the total momentum quadrature  $p_1 + p_2 + p_3$ , whereas more general  $N$ -mode criteria typically contain the weighted combination  $\sum_{i=1}^N g_i p_i$ . Consequently, utilization of such the criterion requires knowledge of all independent elements of the momentum part of the covariance matrix, the number of which scales quadratically with  $N$ . Guided by the effort to detect GME of the largest possible state, we can ask ourselves whether this quadratic growth can be slowed down, e.g., just to the linear growth. Finding a positive answer to this question would undoubtedly be an important result because then the GME certification of some CV states would require a significantly smaller number of measurements. However, such a result would be rather counterintuitive because the respective criterion then could not contain any global combination mentioned above, which might seem to be indispensable for the detection of the global property of the GME.

Interestingly, this intuition is false. Namely, there are two similar criteria of GME, which nevertheless contain variances of combinations of only pairs of position and momentum quadratures. More precisely, one criterion is  $N$ -mode and it is given by [29, Eq. (25)],

$$\sum_{1 \leq i < j \leq N} \langle (x_i + x_j)^2 + (p_i - p_j)^2 \rangle \geq f(N), \quad (2)$$

where  $f(N)$  is a function of  $N$ , whereas the other is four-mode and employs variances of the same combinations (up to the sign) of quadrature operators [37, Eqs. (44) and (47)]. Importantly, both the criteria contain combinations for *all* possible pairs of the modes. Thus as before, the number of the elements of the covariance matrix one needs for application of both the latter criteria grows quadratically with the number of modes  $N$ .

Continuing the same line of thoughts, one can then ask whether the latter criteria are already simplest criteria capable of detecting the GME or their structure can be simplified even further. It is obvious that one cannot simplify the form of the combinations, because they are just two-mode. But since the criteria use the entire covariance matrix of the investigated state, what could be reduced in principle is the number of appearing combinations. Recent results on witnessing qubit GME from separable nearest-neighbour

marginals [41, 42] and their extension to the CV systems [43] indicate that this simplification should be indeed possible.

In this paper we derive such the simplified CV GME criteria for  $N$  modes. Similar to the known criteria also the proposed criteria have the standard form akin to the product and sum uncertainty relation for elements of the covariance matrix and like the criteria [29, Eq. (25)] and [37, Eqs. (44) and (47)] they include at most two-mode quadrature combinations. However, unlike any of the existing CV GME criteria they contain the minimum number of the combinations. The number is minimal because it is equal to the number of elements in the minimal set of two-mode marginal covariance matrices [41, 43], which is needed for detection of GME. Since the number of independent covariance matrix elements contained in the minimal set is equal to  $7N - 4$  [43] and thus grows linearly with  $N$ , the number of elements of the covariance matrix one needs to know for application of the proposed criteria also scales only linearly with  $N$ . As every minimal set can be represented by a tree graph, each of the presented criterion corresponds to a tree. This allowed us to develop a direct method of construction of the criteria, which is based solely on the structure of the underlying tree. We also demonstrate practicality of our criteria by finding analytical as well as numerical examples of Gaussian states whose GME is detected by the criteria for almost all configurations of up to six modes. Interestingly, our criterion detects the GME of a three-mode CV GHZ-like state from its two two-mode reduced density matrices. This is in sharp contrast to the qubit GHZ state for which detection of the GME from two-qubit marginals is impossible [44] and illustrates another difference between discrete and continuous quantum variables.

The proposed criteria are most economic as far as the number of required measurements is concerned and thus they can serve for verification of GME in large multi-mode states. They can be used to detect CV GME even in cases where only the elements of two-mode marginal covariance matrices belonging to some minimal set are available. From a different point of view, the derived criteria can be interpreted in the context of the so-called quantum marginal problem [45, 46]. In its broader sense, this problem addresses the question of determining the presence of some global property based on the knowledge of only a set of reduced density matrices [30, 47]. The task of finding the conditions under which the given reductions are compatible with the property under consideration is then known as the quantum marginal problem. From this perspective, each of the presented criteria can be viewed as a necessary condition for the corresponding minimal set of two-mode covariance matrices having a common global state to be compatible with a biseparable state.

The paper is structured as follows. In Sec. 2 we give

a brief introduction into the concept of GME, whereas Sec. 3 is dedicated to the entanglement in CV systems. Section 4 contains derivation of the minimal criteria for CV GME and the Gaussian GME states which are detected by the criteria are constructed in Sec. 5. Conclusions are in Sec. 6.

## 2 Genuine multipartite entanglement

We deal with  $N$  quantum systems  $1, 2, \dots, N$ , which we collect into the set  $\mathcal{M} = \{1, 2, \dots, N\}$ . Consider further the split of the set  $\mathcal{M}$  into two disjoint nonempty subsets  $I_k = \{i_1, i_2, \dots, i_l\}$ ,  $i_n \in \mathcal{M}$ ,  $n = 1, 2, \dots, l$ ,  $0 < l < N$ , and  $J_k = \mathcal{M} \setminus I_k$ . Here, the index  $k = 1, 2, \dots, K_N$  labels all different inequivalent splits of the set  $\mathcal{M}$  and  $K_N = 2^{N-1} - 1$  is the number of the splits. The splits shall be henceforth called as bipartite splits and denoted as  $I_k|J_k$ . We then say that a state  $\rho$  of the considered system is separable with respect to the split  $I_k|J_k$  if it can be expressed as [1, 2]

$$\rho = \rho_{I_k|J_k}^{\text{sep}} = \sum_i p_i \rho_{I_k}^{(i)} \otimes \rho_{J_k}^{(i)}, \quad (3)$$

where  $\rho_{I_k}^{(i)}$  and  $\rho_{J_k}^{(i)}$  are local states of subsystems belonging to the set  $I_k$  and  $J_k$ , respectively, and  $p_i$  are probabilities. The states which cannot be expressed in the form (3) are then called as entangled with respect to the split and this sort of entanglement is referred to as the bipartite entanglement.

States of systems made up of only two subsystems ( $N = 2$ ) are either entangled or separable, but in systems consisting of more subsystems ( $N > 2$ ) different types of entanglement exist [48, 49]. Various forms of the multipartite entanglement can be illustrated on the system of just three subsystems 1, 2 and 3. In this case, there are three bipartite splits  $1|23$ ,  $2|31$  and  $3|12$ , as well as a tripartite split  $1|2|3$ , and one can classify all states into five separability classes [48, 49] depending on whether they are separable with respect to tripartite split, or only with respect to none, one, two, or three bipartite splits. Clearly, from the point of view of this classification the strongest form of multipartite entanglement is carried by the so-called fully inseparable states, which are entangled across all three bipartite splits.

A specific feature of the most important fully inseparable states, such as the GHZ state, is that global quantum operation on all three subsystems is needed to prepare them. However, this is not a common property of all fully inseparable states. Namely, there is a class of fully inseparable states that can be prepared more easily by randomly mixing states that do not require such a global operation for their preparation [50]. To show this, consider a state  $|\chi\rangle_{ijk} \equiv |\phi_+\rangle_{ij}|0\rangle_k$  of three qubits  $i, j, k$ , where  $|\phi_+\rangle_{ij} = (|00\rangle_{ij} + |11\rangle_{ij})/\sqrt{2}$  is the Bell state, whose

preparation obviously does not need a global three-qubit quantum operation. Let us now imagine that we randomly prepare with the same probability 1/3 one of the states  $|\chi\rangle_{123}, |\chi\rangle_{132}$  and  $|\chi\rangle_{231}$ . Interestingly, the result is also a fully inseparable state [51]. To distinguish states that can be prepared by convex mixing of the product of states with respect to different bipartite splits, called biseparable states [8], from states that cannot be prepared in this way, the concept of GME has been introduced as follows. Generalizing the notion of a biseparable state to  $N$ -partite system,

$$\rho^{\text{bise}} = \sum_{k=1}^{K_N} \lambda_k \rho_{I_k|J_k}^{\text{sep}}, \quad (4)$$

where  $\lambda_j$  are probabilities, we say that a state  $\rho$  is GME, if it cannot be expressed in the form (4).

Genuine multipartite entanglement finds applications in many branches of quantum information science. For this reason, it is desirable to develop efficient GME criteria. Because the set of biseparable states is convex, we can use the machinery of entanglement witnesses [52, 53] for this purpose. In the next section we give a brief introduction into the GME of states of systems with infinite-dimensional Hilbert state spaces and its detection via entanglement witnesses based on second moments.

### 3 Continuous-variable entanglement

We assume that the considered systems  $1, 2, \dots, N$  are the CV systems. Each of the systems is then fully characterized by the position and momentum operators  $x_j$  and  $p_j$  ( $[x_j, p_k] = i\delta_{j,k}$ ),  $j = 1, 2, \dots, N$ , respectively. From now on, we work with the optical platform, where the systems are realized by modes and the position and momentum operators by the respective quadrature operators. It is further convenient to introduce the column vector  $\xi = (\xi_x^T, \xi_p^T)^T$ , where  $\xi_x = (x_1, x_2, \dots, x_N)^T$  and  $\xi_p = (p_1, p_2, \dots, p_N)^T$ , which allows us to express the quadrature commutation rules in the compact form  $[\xi_j, \xi_k] = i(\Omega_N)_{jk}$  with

$$\Omega_N = \begin{pmatrix} \mathbb{O}_N & \mathbb{1}_N \\ -\mathbb{1}_N & \mathbb{O}_N \end{pmatrix}, \quad (5)$$

where  $\mathbb{1}_N$  and  $\mathbb{O}_N$  is the  $N \times N$  identity matrix and zero matrix, respectively. A particularly important class of states of CV systems is given by the so-called Gaussian states, which are defined as states with a Gaussian-shaped Wigner phase-space distribution. For  $N$  modes the states are therefore fully described by the  $2N \times 1$  vector  $\langle \xi \rangle = \text{Tr}(\xi \rho)$  of the first moments and by the  $2N \times 2N$  real symmetric covariance matrix (CM)  $\gamma$  with entries  $(\gamma)_{jk} = \langle \{\Delta \xi_j, \Delta \xi_k\} \rangle$ , where  $\{A, B\} \equiv AB + BA$  is the anticommutator and  $\Delta A \equiv A - \langle A \rangle$ . From the definition of the CM it

further follows that it obeys the uncertainty principle [54]

$$\gamma + i\Omega_N \geq 0. \quad (6)$$

The CM contains information on correlations of the corresponding state and can be used to detect GME by means of the biseparability criterion [33]. It says that if an  $N$ -mode state with CM  $\gamma_{\text{BS}}$  is biseparable, then there exist bipartitions  $I_k|J_k$  and CMs  $\gamma_{I_k} \oplus \gamma_{J_k}$  which are block diagonal with respect to the bipartition  $I_k|J_k$ , and probabilities  $\lambda_k$  such that

$$\gamma_{\text{BS}} - \sum_{k=1}^{K_N} \lambda_k (\gamma_{I_k} \oplus \gamma_{J_k}) \geq 0. \quad (7)$$

If the criterion (7) is violated, the corresponding state is GME. An example of the Gaussian GME state is provided by the CV GHZ-like state [55] with CM

$$\gamma^{\text{GHZ}} = \begin{pmatrix} a_+ & c_+ & c_+ \\ c_+ & a_+ & c_+ \\ c_+ & c_+ & a_+ \end{pmatrix} \oplus \begin{pmatrix} a_- & c_- & c_- \\ c_- & a_- & c_- \\ c_- & c_- & a_- \end{pmatrix}, \quad (8)$$

where

$$a_{\pm} = \frac{e^{\pm 2r} + 2e^{\mp 2r}}{3}, \quad c_{\pm} = \frac{e^{\pm 2r} - e^{\mp 2r}}{3} \quad (9)$$

and  $r \geq 0$  is the squeezing parameter. The GHZ state with CM (8) is also fully inseparable, because the state is pure and for pure states the concepts of GME and full inseparability coincide.

The situation changes for mixed states, where similar to qubits [50] one can find also CV fully inseparable states which are biseparable. One example is given by the manifestly biseparable state  $(\rho_{12}^{\text{TMSV}} \otimes \rho_3^{\text{sq}} + \rho_1^{\text{sq}} \otimes \rho_{23}^{\text{TMSV}})/2$  [26, 36]. Here,  $\rho_i^{\text{sq}}$  is the single-mode squeezed state of mode  $i$  with the squeezing parameter  $r$  and  $\rho_{jk}^{\text{TMSV}}$  is the two-mode squeezed vacuum (TMSV) state of modes  $j$  and  $k$  with CM

$$\gamma_{jk}^{\text{TMSV}} = \begin{pmatrix} a & c \\ c & a \end{pmatrix} \oplus \begin{pmatrix} a & -c \\ -c & a \end{pmatrix}, \quad (10)$$

where  $a = \cosh(2r)$  and  $c = \sinh(2r)$ . An even simpler fully symmetrical example is provided by the state

$$\rho^{\text{test}} = \frac{1}{3} (\rho_{12}^{\text{TMSV}} \otimes |0\rangle_3\langle 0| + \rho_{13}^{\text{TMSV}} \otimes |0\rangle_2\langle 0| + |0\rangle_1\langle 0| \otimes \rho_{23}^{\text{TMSV}}), \quad (11)$$

where all TMSV states have the same squeezing parameter  $r$ . Again, the state is obviously biseparable. Moreover, by applying the positive partial transposition criterion [54] on CM of the state,

$$\gamma^{\text{test}} = \frac{1}{3} (\gamma_{12}^{\text{TMSV}} \oplus \mathbb{1}_3 + \gamma_{13}^{\text{TMSV}} \oplus \mathbb{1}_2 + \mathbb{1}_1 \oplus \gamma_{23}^{\text{TMSV}}), \quad (12)$$

one can show (see Appendix A for details of the calculation) that for  $r \in (0, 1.24)$  the state (11) is at the

same time entangled across all three bipartite splits  $1|23, 2|31$  and  $3|12$ , and thus it is fully inseparable as required.

Both the GHZ-like state with CM (8) as well as the state with CM (11) are simple states suitable for testing of the CV GME criteria. In the following sections we develop such criteria based only on variances of two-mode quadrature combinations and test them, among other things, on these states.

## 4 Minimal criteria for genuine multipartite entanglement

We start by recalling that we look for the GME criteria based on second moments of quadrature operators. Additionally, we restrict ourselves for a while to the sum criteria, for which the left-hand side (LHS) is linear in the second moments. Introducing  $M$  quadrature linear combinations

$$w_i = \sum_{j=1}^{2N} R_{ji} \xi_j, \quad (13)$$

$i = 1, 2, \dots, M$ , where  $R_{ji}$  are elements of a real  $2N \times M$  matrix, the LHS of the criterion then can be expressed for the state with CM  $\gamma$  in the form

$$\sum_{i=1}^M \langle (\Delta w_i)^2 \rangle = \frac{1}{2} \text{Tr} [\gamma R R^T], \quad (14)$$

where the symbol Tr stands for the matrix trace. Further, making use of the structure of biseparable states (4) together with the Cauchy-Schwarz inequality, we can arrive at the following generic form of the necessary condition for biseparability:

$$\text{Tr}[\gamma_{BS} Z] \geq c, \quad (15)$$

for all CMs  $\gamma_{BS}$  of biseparable states. Here,  $Z = R R^T$  is a real, symmetric  $2N \times 2N$  matrix satisfying the condition  $Z \geq 0$  and  $c$  is a non-negative constant which depends on matrix  $R$ . Provided that the matrix  $Z$  has suitable properties and the inequality (15) is violated by some physical CM, the matrix  $Z/c$  can be interpreted as a GME witness in the space of second moments [33, 56]. Expression of the inseparability criterion in terms of the witness matrix is advantageous as it allows us to impose consistently further constraints on its structure, e.g., that the LHS of the criterion contains only the minimal number of two-mode quadrature combinations. In the next subsection we derive such the criteria. The derivation consists of two parts. In the first part, we find the structure of the LHS, whereas in the second part we derive the right-hand side (RHS) of the criterion, which is given by the lower bound on the LHS for all biseparable states.

### 4.1 Left-hand side of the criterion

At the outset we derive the LHS of the sought GME criterion. Similar to other entanglement criteria we rule out combinations mixing position and momentum quadratures by assuming  $Z = Z^x \oplus Z^p$ , where  $Z^x$  and  $Z^p$  are real, symmetric, and positive-semidefinite  $N \times N$  matrices. Inspired by the position part of the criterion (1), which involves combinations  $x_1 - x_2$  and  $x_2 - x_3$ , we further seek the criteria containing the least number of only two-mode quadrature combinations. We therefore require the criteria to utilize only the minimal number of two-mode reduced CMs (marginal CMs), which are needed for detection of GME. The marginal CMs comprise the so-called minimal set of marginals and its structure is already known [41, 43]. The set has to contain all modes and one cannot divide it into a subset and its complement without having a common mode.

A more instructive graphical representation of the minimal set is obtained using the tools of graph theory [57]. Recall, that an undirected graph of order  $N$  is a pair  $G = (V, E)$  of a set  $V = \{1, 2, \dots, N\}$  of  $N$  vertices, and a set  $E \subseteq K \equiv \{(u, v) | (u, v) \in V^2 \wedge u \neq v\}$  of edges. In our case a vertex  $j$  of the graph represents mode  $j$ , whereas the edge connecting adjacent vertices  $j$  and  $k$  represents marginal CM  $\gamma_{jk}$  of modes  $j$  and  $k$ . The minimal set of marginals is then represented by an undirected connected graph containing no cycles, also known as an unlabeled tree [58], which shall be henceforth denoted as  $T$ . Here, we are interested in the GME which exists in systems of at least three modes and we therefore assume  $N \geq 3$  from now. A closed formula for the number of non-isomorphic trees of order  $N$  is not known, yet it is known to grow exponentially [59]. For small  $N$  the number can be found in Ref. [60], and in particular, for  $N = 3, 4, 5, 6, \dots$ , there is  $1, 2, 3, 6, \dots$ , non-isomorphic unlabeled trees.

In the next step we imprint the structure of the respective minimal set of marginals on the LHS of the required criterion. This can be done elegantly with the help of the adjacency matrix of a graph  $G$ , denoted as  $A$ , which is an  $N \times N$  symmetric matrix in which entry  $A_{jk}$  is the number of edges in  $G$  connecting vertices  $j$  and  $k$ . Since a tree is a simple graph with no loops or multiple edges, its adjacency matrix is a zero-one matrix with zeros on the diagonal [57]. In order the criterion to use only the minimal set of marginals corresponding to a tree with adjacency matrix  $A$ , its matrices denoted as  $Z_A^x$  and  $Z_A^p$  have to have generally non-zero diagonal elements and zero off-diagonal elements on the same places as the matrix  $A$ . This is simply achieved by the matrices

$$Z_A^{x,p} = (\mathbb{1}_N + A) \circ Z^{x,p}, \quad (16)$$

where  $X \circ Y$  is the Hadamard (elementwise) matrix product with entries  $(X \circ Y)_{jk} = X_{jk} Y_{jk}$  [61] and  $Z^{x,p}$  are some real symmetric matrices with no zero entries. The LHS of the required criterion corresponding to a

minimal set of marginal CMs with adjacency matrix  $A$  thus possesses the following structure:

$$\text{Tr}[\gamma Z_A] = \text{Tr}[\gamma^x Z_A^x] + \text{Tr}[\gamma^p Z_A^p]. \quad (17)$$

Here  $Z_A^{x,p}$  are some real, symmetric, and positive-semidefinite matrices of the form (16), and  $\gamma^x$  and  $\gamma^p$  is the first and second  $N \times N$  diagonal block of the CM  $\gamma$  with entries  $(\gamma^x)_{jk} = \langle \{\Delta x_j, \Delta x_k\} \rangle$  and  $(\gamma^p)_{jk} = \langle \{\Delta p_j, \Delta p_k\} \rangle$ , respectively.

It remains to rewrite the RHS of Eq. (17) in terms of variances of two-mode quadrature combinations. Since the witness matrices  $Z_A^{x,p}$  are always real, symmetric and positive-semidefinite, one can use the Cholesky decomposition and express them as  $Z_A^\alpha = L_A^\alpha (L_A^\alpha)^T$ , where  $L_A^\alpha$ ,  $\alpha = x, p$ , are real lower triangular  $N \times N$  matrices with non-negative diagonal elements [62–64]. Like in the case of the matrix  $Z_A^\alpha$  the structure of the Cholesky matrix  $L_A^\alpha$  also depends on the respective adjacency matrix  $A$ , which is expressed by the lower index  $A$ . In what follows, the lower index is dropped for brevity, i.e., from now by the symbol  $L^\alpha$  we understand a Cholesky matrix corresponding to some adjacency matrix  $A$ .

Making further use of the cyclic property of the matrix trace and the definition of a CM we then get

$$\begin{aligned} \text{Tr}[\gamma^\alpha Z_A^\alpha] &= \text{Tr}[\gamma^\alpha L^\alpha (L^\alpha)^T] \\ &= 2 \sum_{i=1}^N \langle \{\Delta[(L^\alpha)^T \xi_\alpha]_i\}^2 \rangle \\ &= 2 \sum_{i=1}^N \langle (\Delta u_i^\alpha)^2 \rangle \equiv 2U^\alpha, \end{aligned} \quad (18)$$

$\alpha = x, p$ . Here we introduced the multi-mode position and momentum variables,

$$u_i^x \equiv \sum_{j=i}^N L_{ji}^x x_j, \quad u_i^p \equiv \sum_{j=i}^N L_{ji}^p p_j, \quad (19)$$

$i = 1, \dots, N$ , and sums of their variances,

$$U^x \equiv \sum_{i=1}^N \langle (\Delta u_i^x)^2 \rangle, \quad U^p \equiv \sum_{i=1}^N \langle (\Delta u_i^p)^2 \rangle. \quad (20)$$

Similar to other entanglement criteria we then define the LHS of our criterion as one half of the expression (17), i.e.,  $U^x + U^p$ . However, in the present case each of the quantities  $U^\alpha$ ,  $\alpha = x, p$ , contains  $N$  variances of the quadrature combinations of the form (19).

In general, the LHS will not still possess the desired form containing variances of at most two-mode quadrature combinations. Namely, for  $i = 1, 2, \dots, N-2$  the operators (19) contain generally  $N-i+1 \geq 2$  terms and not at most two, as required. Interestingly, also all these combinations can attain the required structure, at least for some trees, if we label suitably vertices of the tree representing

the considered minimal set of marginal CMs. The labeling can be found in several steps.

At the outset we show how the requirement that quadrature combinations (19) contain at most two terms manifests itself on the level of the respective adjacency matrix  $A$ . Recall first, that we seek a necessary condition for biseparability of the form  $f_\gamma(L^x, L^p) \geq g(L^x, L^p)$ . On the LHS there is a function  $f_\gamma(L^x, L^p)$  which depends on CM  $\gamma$  of the tested state and Cholesky matrices  $L^{x,p}$  of some witness matrices  $Z_A^{x,p}$ . The RHS of the condition, which we derive in the next section, imposes a lower bound on the LHS for all biseparable states, and it is formed by a function  $g(L^x, L^p)$  depending only on the matrices  $L^{x,p}$ . The biseparability condition then can be used for testing of the presence of GME in a given CM  $\gamma$  by numerical minimization of the difference  $f_\gamma(L^x, L^p) - g(L^x, L^p)$  over the matrices  $L^{x,p}$ . If the minimum is negative, i.e., the biseparability condition is violated, then the state with CM  $\gamma$  is inevitably GME. Here, we are interested only in a generic form of the biseparability condition capable of detecting the largest number of GME states from a minimal set of marginal CMs. Clearly, such a condition is obtained if the function  $f_\gamma(L^x, L^p)$  depends on the maximum number of independent variables, i.e., if the Cholesky matrices  $L^{x,p}$  corresponding to the minimal set have the maximum number of non-zero elements. Working with the positive-semidefinite matrices  $Z_A^{x,p}$ , we would have to take into account that some diagonal elements of the Cholesky matrices  $L^{x,p}$  can be equal to zero [64, p. 8.3] thereby reducing the number of the variables over which we will optimize. For this reason we assume from now that the matrices  $Z_A^{x,p}$  are positive-definite which implies that the corresponding Cholesky matrices  $L^{x,p}$  possess strictly positive diagonal elements which can be expressed as [63, Theorem 4.2.5]

$$L_{11}^\alpha = \sqrt{(Z_A^\alpha)_{11}}, \quad L_{ii}^\alpha = \sqrt{(Z_A^\alpha)_{ii} - \sum_{j=1}^{i-1} (L_{ij}^\alpha)^2}, \quad (21)$$

$i = 2, 3, \dots, N$ .

Now, let us rewrite the first  $N-1$  combinations (19) in the compact form

$$\begin{aligned} u_i^x &= x_i L_{ii}^x + (x_{i+1}, x_{i+2}, \dots, x_N) \cdot L_{i+1:N,i}^x, \\ u_i^p &= p_i L_{ii}^p + (p_{i+1}, p_{i+2}, \dots, p_N) \cdot L_{i+1:N,i}^p, \end{aligned} \quad (22)$$

$i = 1, 2, \dots, N-1$ , where the symbol “ $\cdot$ ” stands for the scalar product and

$$L_{i+1:N,i}^\alpha \equiv (L_{i+1,i}^\alpha, L_{i+2,i}^\alpha, \dots, L_{N,i}^\alpha)^T \quad (23)$$

are  $(N-i) \times 1$  column vectors comprising lower triangular part without the main diagonal of the matrix  $L^\alpha$ . Hence, we see that the operators (22) will contain at most two non-zero terms if each of the vectors  $L_{i+1:N,i}^\alpha$  will have at most one non-zero component.

In the Appendix B we show that this will be the case if all vectors  $(Z_A^\alpha)_{i+1:N,i}$ ,  $i = 1, 2, \dots, N-1$  will possess at most one non-zero component and the vector (23) is the given by

$$L_{i+1:N,i}^\alpha = \frac{(Z_A^\alpha)_{i+1:N,i}}{L_{ii}^\alpha}. \quad (24)$$

Making further use of the formula (16) we can write

$$(Z_A^\alpha)_{i+1:N,i} = A_{i+1:N,i} \circ (Z^\alpha)_{i+1:N,i}, \quad (25)$$

which leads, when combined with Eq. (24), to the final formula for the Cholesky matrices of the sought criterion,

$$L^\alpha = (\mathbb{1}_N + A) \circ \ell^\alpha, \quad (26)$$

where  $\ell^\alpha$  is a lower triangular matrix with non-zero entries and strictly positive diagonal elements. Ascertaining of the structure of the adjacency matrix  $A$ , which leads to the quadrature combinations (19) with at most two non-zero terms, is now simple. The quadrature combinations (19) then contain only  $4N - 2$  elements. From the formula (25) it follows immediately that this happens if the vectors  $A_{i+1:N,i}$ ,  $i = 1, 2, \dots, N-1$ , contain only one non-zero element. As the structure of the adjacency matrix is for a given tree dictated by the labeling of its vertices, the question of the possibility to have a GME criterion based only on at most two-mode quadrature combinations boils down to the question of the existence of the tree labeling which would possess in each vector  $A_{i+1:N,i}$  only one non-zero component. In what follows we show that such a labeling really exists, at least for some trees.

#### 4.1.1 Linear tree

The first example of a tree for which the labeling is easy to find is an  $N$ -vertex linear tree. Consider the standard labeling of the vertices by natural numbers in an increasing order from the leftmost vertex to the rightmost vertex as exemplified in Fig. 1 a) (see also labeled trees in the second, fourth and seventh row of Tab. 3 for examples corresponding to  $N = 4, 5$  and 6). The corresponding adjacency matrix has elements  $A_{ij} = \delta_{|i-j|,1}$ ,  $i, j = 1, 2, \dots, N$ , for which the quantities (20) are given by

$$U_{\text{lin}}^\alpha = \sum_{i=1}^{N-1} \langle [\Delta(\ell_{ii}^\alpha \alpha_i + \ell_{i+1,i}^\alpha \alpha_{i+1})]^2 \rangle + (\ell_{NN}^\alpha)^2 \langle (\Delta \alpha_N)^2 \rangle, \quad (27)$$

$\alpha = x, p$ , where the relations (19), (20) and (26) have been used. Clearly, the RHS of the latter formula consists of variances of at most two-mode quadrature combinations as required. Note further, that the presented labeling is not the only one for which the LHS of the criterion attains the desired form. For instance, it is easy to show that for the so-called reverse level

order labeling introduced below in this paper and depicted for a linear tree in Fig. 1 b), the sums (20) also contain variances of at most two-mode quadrature combinations.



Figure 1: Four-mode example of the standard labeling a) and the alternative reverse level order labeling b) of a linear tree, which yields the quantities (20) with variances of quadrature combinations (19) containing at most two terms.

#### 4.1.2 Star tree

Let us now move to the  $N$ -vertex star tree. We see that the labeling we are looking for is established if we label the central vertex with  $N$  and the other vertices are labeled by the natural numbers  $N-1, N-2, \dots, 1$  in a decreasing order in the anticlockwise direction (see labeled trees in the third, fifth and eighth row of Tab. 3 for examples corresponding to  $N = 4, 5$  and 6). For this labeling the only non-zero elements of the adjacency matrix are  $A_{Ni} = A_{iN} = 1$ , and they yield sums (20) of the following form:

$$U_{\text{star}}^\alpha = \sum_{i=1}^{N-1} \langle [\Delta(\ell_{ii}^\alpha \alpha_i + \ell_{Ni}^\alpha \alpha_N)]^2 \rangle + (\ell_{NN}^\alpha)^2 \langle (\Delta \alpha_N)^2 \rangle, \quad (28)$$

$\alpha = x, p$ . Again, the LHS of the corresponding criterion comprise variances of at most two-mode quadrature combinations.

#### 4.1.3 Generic tree

Interestingly, even generic trees can be labeled such, at least for low orders, i.e., low  $N$ , that the corresponding quadrature combinations (19) contain at most two non-zero terms. This can be done as follows.

Let us start by recalling that the degree of a vertex in a graph is the number of edges incident to it and that a vertex of degree one is called as a leaf. Consider now a tree  $T$  and imagine an iterative procedure [57, 65] in which in each step we delete all leaves of the tree obtained in the previous step. At the end, we are left either with a single vertex or a single edge, which is the so-called center of the tree  $T$  (see Tab. 1 for examples of both the instances). Alternatively, we get the center by taking a vertex or an edge which lies in the middle of any longest path in the tree [65]. Next, if the center of the tree is a vertex, we choose it as the so-called root of the tree, whereas if it is an edge, we choose one of its endpoints as a root (see red vertices in Tab. 1). Having established a root, we now associate with each vertex a level which is the number of edges from the vertex to the root and arrange the vertices into horizontal layers, where in

Table 1: Examples of the reverse level order labeling for generic trees. The trees are rooted by selecting a central vertex or one endpoint of the central edge as a root (red vertices). The vertices are then labeled by natural numbers in a decreasing order starting by labeling the root with  $N$  and then going from level to level, where in each level the vertices are labeled consecutively from left to right.

$N$	Unlabeled tree	Type of center	Rooted tree
7		vertex	
7		edge	
8		edge	

the topmost layer there is only the root, the second layer is comprised of level-one vertices etc. (see the last column of Tab. 1). This allows us to introduce a labeling of the tree  $T$ , which can be called fittingly as a reverse level order labeling. Here, we label the vertices by natural numbers in a decreasing order starting by assigning the label  $N$  to the root and continuing level by level going from left to right at each level (see the last column of Tab. 1, as well as the third column of Tab. 3 for explicit examples).

We checked by a direct calculation that for all configurations of up to  $N = 10$  the established reverse level order labeling leads to an adjacency matrix, where each vector  $A_{i+1:N,i}$  contains only one non-zero component and therefore the respective quadrature combinations (19) contain at most two non-zero terms. This leads us to a conjecture that this statement holds generally for an arbitrary  $N$ -vertex tree.

Note finally that the reverse level order labeling is not the only labeling yielding vectors  $A_{i+1:N,i}$ ,  $i = 1, 2, \dots, N-1$ , each with only one non-zero component. Other labeling equipped with the same property is the “natural” labeling of a linear tree exemplified in the preceding subsubsection or the labeling of a tree depicted in Fig. 2.

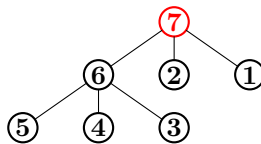


Figure 2: Example of a tree labeling which is different from the reverse level order labeling displayed in the second row of Tab. 1, yet it leads to the GME criterion with at most two-mode quadrature combinations (19). See text for details.

## 4.2 Right-hand side of the criterion

In the next step, we find a lower bound for the LHS of the sought criterion, which we obtained in the preceding subsection. Following the standard approach [36], we find a lower bound both on the sum  $U^x + U^p$  and on the product  $U^x U^p$  for all biseparable states. Thus we get two necessary conditions for biseparability, which we call the sum condition and the product condition, respectively. Negation of the conditions then yields two sufficient conditions for GME. Below we give examples of GME states detected by both the criteria, as well as by only one of them, which demonstrates that they certify GME of intersecting but generally different sets of states.

In what follows we first derive a product necessary condition for biseparability and then we continue with derivation of the sum condition.

### 4.2.1 Product criterion

Our goal is to find a lower bound for the product

$$U^x U^p = \sum_{i,j=1}^N \langle (\Delta u_i^x)^2 \rangle \langle (\Delta u_j^p)^2 \rangle, \quad (29)$$

where

$$u_i^\alpha = \sum_{j=1}^N L_{ji}^\alpha \alpha_j, \quad (30)$$

$\alpha = x, p$ , for all biseparable states (4). Contrary to Eq. (19), in Eq. (30) we for simplicity do not take into account explicitly the fact that  $L_{ji}^\alpha = 0$  for  $j < i$ .

Note first, that the product (29) is lower bounded as

$$\begin{aligned} U^x U^p &\stackrel{1}{\geq} \left( \sum_{k=1}^{K_N} \lambda_k U_k^x \right) \left( \sum_{l=1}^{K_N} \lambda_l U_l^p \right) \\ &\stackrel{2}{\geq} \left( \sum_{k=1}^{K_N} \lambda_k \sqrt{U_k^x U_k^p} \right)^2, \end{aligned} \quad (31)$$

with

$$U_k^\alpha \equiv \sum_{i=1}^N \langle (\Delta u_i^\alpha)^2 \rangle_{\rho_{I_k|J_k}^{\text{sep}}}, \quad (32)$$

$\alpha = x, p$ , where the symbol  $\langle \rangle_\rho$  stands for the mean in the state  $\rho$ . Here, to get inequality 1 we used the concavity of the variance with respect to convex mixtures [66], which we applied to the mixture  $\rho^{\text{bise}}$ , Eq. (4), whereas inequality 2 follows from the Cauchy-Schwarz inequality.

Next, we lower bound the product

$$U_k^x U_k^p = \sum_{i,j=1}^N \langle (\Delta u_i^x)^2 \rangle_{\rho_{I_k|J_k}^{\text{sep}}} \langle (\Delta u_j^p)^2 \rangle_{\rho_{I_k|J_k}^{\text{sep}}}. \quad (33)$$

For this purpose, consider a bipartite split  $k \equiv I_k|J_k$ , where  $I_k = \{i_1, i_2, \dots, i_l\}$  and  $J_k =$

$\{i_{l+1}, i_{l+2}, \dots, i_N\}$ , and assume that the system is prepared in the separable state  $\rho_{I_k|J_k}^{\text{sep}}$ , Eq. (3). Let as further decompose the operators (30) into two parts, one belonging to the subsystem  $I_k$  and the other to the subsystem  $J_k$ ,

$$u_i^\alpha = u_{i,I_k}^\alpha + u_{i,J_k}^\alpha, \quad (34)$$

where

$$u_{i,I_k}^\alpha \equiv \sum_{n=1}^l L_{i_n i}^\alpha \alpha_{i_n}, \quad u_{i,J_k}^\alpha \equiv \sum_{n=l+1}^N L_{i_n i}^\alpha \alpha_{i_n}. \quad (35)$$

Inspired by the approach of Ref. [27] we can then lower bound the variance product appearing on the RHS of Eq. (33) as

$$\begin{aligned} & \langle (\Delta u_i^x)^2 \rangle_{\rho_{I_k|J_k}^{\text{sep}}} \langle (\Delta u_j^p)^2 \rangle_{\rho_{I_k|J_k}^{\text{sep}}} \\ & \stackrel{1}{\geq} \left[ \sum_l p_l^{(k)} \langle (\Delta u_i^x)^2 \rangle_{\rho_{I_k \otimes J_k}^{(l)}} \right] \left[ \sum_m p_m^{(k)} \langle (\Delta u_j^p)^2 \rangle_{\rho_{I_k \otimes J_k}^{(m)}} \right] \\ & \stackrel{2}{\geq} \left[ \sum_l p_l^{(k)} \sqrt{\langle (\Delta u_i^x)^2 \rangle_{\rho_{I_k \otimes J_k}^{(l)}} \langle (\Delta u_j^p)^2 \rangle_{\rho_{I_k \otimes J_k}^{(l)}}} \right]^2 \\ & \stackrel{3}{\geq} \left\{ \sum_l p_l^{(k)} \left[ \sqrt{\langle (\Delta u_{i,I_k}^x)^2 \rangle_{\rho_{I_k}^{(l)}} \langle (\Delta u_{j,I_k}^p)^2 \rangle_{\rho_{I_k}^{(l)}}} \right. \right. \\ & \quad \left. \left. + \sqrt{\langle (\Delta u_{i,J_k}^x)^2 \rangle_{\rho_{J_k}^{(l)}} \langle (\Delta u_{j,J_k}^p)^2 \rangle_{\rho_{J_k}^{(l)}}} \right] \right\}^2 \\ & \stackrel{4}{\geq} \frac{1}{4} \left\{ \left| [(L^x)^T L^p]_{ij}^{(I_k)} \right| + \left| [(L^x)^T L^p]_{ij}^{(J_k)} \right| \right\}^2 \\ & \stackrel{5}{=} \frac{1}{4} \left\{ [(L^x)^T L^p]_{ij}^2 + 2(|X_{ij}^{(k)}| - X_{ij}^{(k)}) \right\}, \end{aligned} \quad (36)$$

where we introduced the denotation  $\rho_{I_k \otimes J_k}^{(l)} \equiv \rho_{I_k}^{(l)} \otimes \rho_{J_k}^{(l)}$ . Here, inequality 1 follows from concavity of the variance, inequality 2 is a consequence of the Cauchy-Schwarz inequality and inequality 3 results from the averaging in the product state  $\rho_{I_k \otimes J_k}^{(l)}$  and again the Cauchy-Schwarz inequality. Finally, in inequality 4 we used the uncertainty relations and the quantities appearing on the RHS of the inequality and equality 5 are defined as

$$[(L^x)^T L^p]_{ij}^{(I_k)} \equiv \sum_{n=1}^l [(L^x)^T]_{ii_n} L_{i_n j}^p, \quad (37)$$

$$[(L^x)^T L^p]_{ij}^{(J_k)} \equiv \sum_{n=l+1}^N [(L^x)^T]_{ii_n} L_{i_n j}^p, \quad (38)$$

$$X_{ij}^{(k)} \equiv [(L^x)^T L^p]_{ij}^{(I_k)} [(L^x)^T L^p]_{ij}^{(J_k)}. \quad (39)$$

Combining now Eq. (33) with inequality (36) we get immediately the following inequality

$$U_k^x U_k^p \geq \frac{1}{4} (\mathcal{L} + \mathcal{L}^{(k)}), \quad (40)$$

where

$$\mathcal{L} \equiv \sum_{i,j=1}^N [(L^x)^T L^p]_{ij}^2, \quad (41)$$

$$\mathcal{L}^{(k)} \equiv 2 \sum_{i,j=1}^N (|X_{ij}^{(k)}| - X_{ij}^{(k)}). \quad (42)$$

Finally, putting inequalities (31) and (40) together, we arrive at the sought necessary condition for biseparability of the form:

$$U^x U^p \geq \frac{1}{4} \left\{ \mathcal{L} + \min \left[ \mathcal{L}^{(1)}, \dots, \mathcal{L}^{(2^{N-1}-1)} \right] \right\}, \quad (43)$$

where we used the fact that  $K_N = 2^{N-1} - 1$ .

#### 4.2.2 Sum criterion

Derivation of the sum condition is simpler. First, we use concavity of the variance to get

$$U^x + U^p \geq \sum_{i=1}^N \sum_{k=1}^{K_N} \lambda_k \sum_{\alpha=x,p} \langle (\Delta u_i^\alpha)^2 \rangle_{\rho_{I_k|J_k}^{\text{sep}}}. \quad (44)$$

Next, we lower bound the sum of the variances on the RHS as

$$\begin{aligned} & \sum_{\alpha=x,p} \langle (\Delta u_i^\alpha)^2 \rangle_{\rho_{I_k|J_k}^{\text{sep}}} \\ & \stackrel{1}{\geq} \sum_{\alpha=x,p} \sum_l p_l^{(k)} \langle (\Delta u_i^\alpha)^2 \rangle_{\rho_{I_k \otimes J_k}^{(l)}} \\ & \stackrel{2}{=} \sum_{\alpha=x,p} \sum_l p_l^{(k)} \left[ \langle (\Delta u_{i,I_k}^\alpha)^2 \rangle_{\rho_{I_k}^{(l)}} + \langle (\Delta u_{i,J_k}^\alpha)^2 \rangle_{\rho_{J_k}^{(l)}} \right] \\ & \stackrel{3}{\geq} \left| [(L^x)^T L^p]_{ii}^{(I_k)} \right| + \left| [(L^x)^T L^p]_{ii}^{(J_k)} \right|, \end{aligned} \quad (45)$$

where inequality 1 again follows from concavity of the variance, whereas in equality 2 we used the decomposition (34) and the fact that we average over the product state  $\rho_{I_k \otimes J_k}^{(l)}$ . To get inequality 3 we used the inequality between the arithmetic and geometric mean, the uncertainty relations, and the definitions (37) and (38). Finally, if we combine inequalities (44) and (45) we obtain the desired sum criterion in the following form:

$$U^x + U^p \geq \min \left[ \mathcal{K}^{(1)}, \dots, \mathcal{K}^{(2^{N-1}-1)} \right], \quad (46)$$

where

$$\mathcal{K}^{(k)} \equiv \sum_{i=1}^N \left\{ \left| [(L^x)^T L^p]_{ii}^{(I_k)} \right| + \left| [(L^x)^T L^p]_{ii}^{(J_k)} \right| \right\}. \quad (47)$$

Testing of the presence of GME in a given quantum state by means of the criteria (43) and (46) requires to find a set of parameters  $\ell_{ij}^\alpha$ , for which the respective

inequalities (43) and (46) are violated. This can be done by minimization of the difference

$$D_P \equiv U^x U^p - \frac{1}{4} \left\{ \mathcal{L} + \min \left[ \mathcal{L}^{(1)}, \dots, \mathcal{L}^{(2^{N-1}-1)} \right] \right\} \quad (48)$$

or

$$D_S \equiv U^x + U^p - \min \left[ \mathcal{K}^{(1)}, \dots, \mathcal{K}^{(2^{N-1}-1)} \right] \quad (49)$$

over the parameters  $\ell_{ij}^\alpha$ . Clearly, if the difference is negative, the investigated state is GME.

In the next Section we use this approach to verify GME in several multi-mode quantum states. This requires to select a certain tree and express the respective differences (48) and (49) in terms of the parameters  $\ell_{ij}^\alpha$  by means of the formula (26). This can be rather cumbersome, in particular, for trees with many vertices. For this reason, it is desirable to develop a simpler construction of the criteria, which would ideally utilize only the structure of the considered tree. In the following subsection we present such a construction for the sum criterion.

### 4.3 Direct construction of the sum criterion

Practical utility of the proposed criteria would be significantly increased if we would be able to construct them directly from the underlying tree. While construction of the LHS for both the criteria is the same, construction of the RHS is transparent only for the sum criterion. Below, we therefore construct the RHS for the sum criterion, whereas the construction for the product criterion is deferred for further research.

#### 4.3.1 Construction of the left-hand side

The quantities  $U^{x,p}$ , Eq. (20), on the LHS of both criteria are the same and their construction is easy. Namely, each  $N$ -vertex tree consists of  $N-1$  edges [57]. Each of the edges connects a pair of vertices with labels  $i$  and  $j$ , where by  $i$  we denote the label which is less than the label  $j$ , i.e.,  $i < j$ . With each of the edges we associate a two-mode quadrature linear combination  $u_i^\alpha$  (see Fig. 3). Sum of the variances  $\langle (\Delta u_i^\alpha)^2 \rangle$  over all edges then comprises (up to the term  $(\ell_{NN}^\alpha)^2 \langle (\Delta \alpha_N)^2 \rangle$ ) the quantity  $U^\alpha$ . More

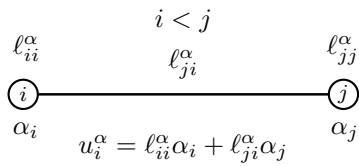


Figure 3: Construction of the two-mode quadrature combination  $u_i^\alpha$  corresponding to the edge  $e_{ij} = ij$  connecting vertices  $i$  and  $j$ . See text for details.

precisely, to each vertex  $i$  we ascribe the quadrature  $\alpha_i$ , as well as the diagonal element  $\ell_{ii}^\alpha$  of the matrix

$\ell^\alpha$ . Next, to each edge connecting the vertices  $i$  and  $j$  we assign the off-diagonal entry  $\ell_{ji}^\alpha$ . The edge is then represented by the quadrature combination

$$u_i^\alpha = \ell_{ii}^\alpha \alpha_i + \ell_{ji}^\alpha \alpha_j. \quad (50)$$

The quantity  $U^\alpha$  in Eq. (20) is then given by the sum of variances of all  $N-1$  quantities (50), plus the term  $(\ell_{NN}^\alpha)^2 \langle (\Delta \alpha_N)^2 \rangle$ . Making use of this rule we can easily rederive the quantities  $U^\alpha$  for the linear tree and the star tree given in Eqs. (27) and (28), respectively. In the next section we also use the rule to construct the criteria corresponding to the more complex trees in the third column of Tab. 3.

#### 4.3.2 Construction of the right-hand side

Construction of the RHS of the sum criterion is also easy. Recall first, that in a tree with root  $N$  there is for each vertex  $i$  a unique  $i, N$ -path. The so-called parent of vertex  $i$  is an adjacent vertex on the  $i, N$ -path [57] and each non-root vertex has exactly one parent. Let  $j$  be the label of the parent of vertex  $i$ , where inequality  $i < j$  always holds in our labeling, and  $e_{ij} \equiv ij$  be the edge joining the vertex  $i$  with its parent  $j$ . Now, for each non-root vertex  $i$  we create a pair  $(i, e_{ij})$  and represent it by the pair  $(\ell_{ii}^x \ell_{ii}^p, \ell_{ji}^x \ell_{ji}^p)$  of products of elements of matrices  $\ell^{x,p}$ , which are associated with the vertex  $i$  and the edge  $e_{ij}$  according to Fig. 3. The root  $N$  has no parent and thus there is no edge associated to it. Therefore, it is represented just by the term  $\ell_{NN}^x \ell_{NN}^p$ .

Moving to the construction of the RHS it is obvious that to every bipartite split  $k \equiv I_k | J_k$  of  $N$  modes into two disjoint subsets  $I_k = \{i_1, i_2, \dots, i_l\}$  and  $J_k = \{i_{l+1}, i_{l+2}, \dots, i_N\}$  there corresponds exactly the same bipartite split of the set of all  $N$  vertices of the considered graph. The split divides the set of all  $N-1$  pairs  $(i, e_{ij})$  into two disjoint subsets, denoted as  $\mathcal{U}$  and  $\mathcal{C}$ , depending on whether the edge  $e_{ij}$  is uncut by the split or it is cut off by the split. Formally,  $(i, e_{ij}) \in \mathcal{U}$  if  $i, j \in I_k$  or  $i, j \in J_k$ , whereas  $(i, e_{ij}) \in \mathcal{C}$  if  $i \in I_k$  and  $j \in J_k$  or vice versa. Now, to each pair  $(i, e_{ij}) \in \mathcal{U}$  we ascribe the term  $|\ell_{ii}^x \ell_{ii}^p + \ell_{ji}^x \ell_{ji}^p|$ , whereas with each pair  $(i, e_{ij}) \in \mathcal{C}$  we associate a different term  $|\ell_{ii}^x \ell_{ii}^p| + |\ell_{ji}^x \ell_{ji}^p|$ . The sum of all the latter terms for all  $N-1$  pairs  $(i, e_{ij})$  plus the term  $|\ell_{NN}^x \ell_{NN}^p|$ , which corresponds to the root, gives finally the quantity  $\mathcal{K}^{(k)}$ , Eq. (47), appearing on the RHS of the sum criterion (46).

Explicit construction of all the quantities  $\mathcal{K}^{(k)}$  for the simplest case of  $N=3$  modes is presented in Fig. 4.

## 5 Applications

### 5.1 Three-mode states

First, we test functionality of the product criterion (43) and sum criterion (46) for the simplest case of

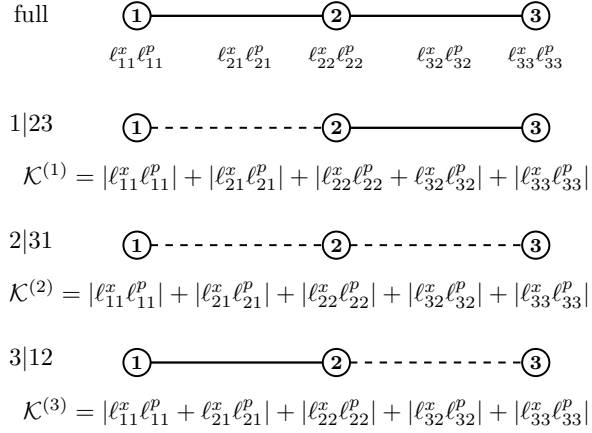


Figure 4: Graphical construction of the quantities  $\mathcal{K}^{(k)}$ ,  $k = 1, 2, 3$ , appearing on the RHS of the sum criterion (46) for the 3-vertex tree with the standard labeling (uppermost graph). The lower graphs correspond consecutively to the full tree after the cuts with respect to bipartite splits  $1 \equiv 1|23$ ,  $2 \equiv 2|31$  and  $3 \equiv 3|12$ . The uncut edges are represented by solid lines, whereas the cut off edges by the dashed lines. See text for details.

$N = 3$  modes. Then there is only one linear tree which for the standard labeling yields the adjacency matrix given above Eq. (27). Hence, one gets using the formula (41)

$$\begin{aligned} \mathcal{L} = & (\ell_{11}^x \ell_{11}^p + \ell_{21}^x \ell_{21}^p)^2 + (\ell_{21}^x \ell_{22}^p)^2 + (\ell_{22}^x \ell_{21}^p)^2 \\ & + (\ell_{22}^x \ell_{22}^p + \ell_{32}^x \ell_{32}^p)^2 + (\ell_{32}^x \ell_{33}^p)^2 + (\ell_{33}^x \ell_{32}^p)^2 \\ & + (\ell_{33}^x \ell_{33}^p)^2. \end{aligned} \quad (51)$$

The three modes can be divided into three bipartite splits which we denote as  $1 \equiv 1|23$ ,  $2 \equiv 2|31$  and  $3 \equiv 3|12$ , and for the splits we further obtain

$$\begin{aligned} \mathcal{L}^{(1)} = & 2(|\ell_{11}^x \ell_{11}^p \ell_{21}^x \ell_{21}^p| - \ell_{11}^x \ell_{11}^p \ell_{21}^x \ell_{21}^p), \\ \mathcal{L}^{(3)} = & 2(|\ell_{22}^x \ell_{22}^p \ell_{32}^x \ell_{32}^p| - \ell_{22}^x \ell_{22}^p \ell_{32}^x \ell_{32}^p), \\ \mathcal{L}^{(2)} = & \mathcal{L}^{(1)} + \mathcal{L}^{(3)}, \end{aligned} \quad (52)$$

by Eq. (42). Making use of the expressions for the quantities  $U_{\text{lin}}^{x,p}$ , Eq. (27), we get finally the minimal three-mode product criterion for GME,

$$\begin{aligned} \prod_{\alpha=x,p} \left\{ \sum_{i=1}^2 \langle [\Delta(\ell_{ii}^\alpha \alpha_i + \ell_{i+1i}^\alpha \alpha_{i+1})]^2 \rangle \right. \\ \left. + (\ell_{33}^\alpha)^2 \langle (\Delta \alpha_3)^2 \rangle \right\} \\ \geq \frac{1}{4} \left\{ \mathcal{L} + \min \left[ \mathcal{L}^{(1)}, \mathcal{L}^{(2)}, \mathcal{L}^{(3)} \right] \right\}. \end{aligned} \quad (53)$$

Moving to the sum criterion (46) for three modes, the product on the LHS of the latter inequality is replaced with the sum, whereas the quantities  $\mathcal{K}^{(k)}$  appearing on the RHS were derived in Fig. 4. Additionally, since  $\mathcal{K}^{(1)}, \mathcal{K}^{(3)} \leq \mathcal{K}^{(2)}$ , it is sufficient to take only  $\min\{\mathcal{K}^{(1)}, \mathcal{K}^{(3)}\}$  on the RHS of the considered criterion. Putting it all together the minimal

three-mode sum criterion for GME reads as

$$\begin{aligned} \sum_{\alpha=x,p} \left\{ \sum_{i=1}^2 \langle [\Delta(\ell_{ii}^\alpha \alpha_i + \ell_{i+1i}^\alpha \alpha_{i+1})]^2 \rangle \right. \\ \left. + (\ell_{33}^\alpha)^2 \langle (\Delta \alpha_3)^2 \rangle \right\} \\ \geq \min (|\ell_{11}^x \ell_{11}^p| + |\ell_{21}^x \ell_{21}^p| + |\ell_{22}^x \ell_{22}^p| + |\ell_{32}^x \ell_{32}^p| \\ + |\ell_{33}^x \ell_{33}^p|, |\ell_{11}^x \ell_{11}^p + \ell_{21}^x \ell_{21}^p| + |\ell_{22}^x \ell_{22}^p| \\ + |\ell_{32}^x \ell_{32}^p| + |\ell_{33}^x \ell_{33}^p|). \end{aligned} \quad (54)$$

At the outset we confirm on a particular example that a fully inseparable but not GME state really does not violate the inequalities (53) and (54). As an example we use the family of fully inseparable biseparable states (11) with CM  $\gamma^{\text{test}}$ , Eq. (12), where  $r \in (0, 1.24)$ . For all states with the squeezing parameter  $r_i = 0.05 \times i$ ,  $i = 0, 1, \dots, 24$ , we have minimized numerically the differences  $D_P$  and  $D_S$ , Eqs. (48) and (49) with  $N = 3$ , i.e., the difference of the LHS and the RHS of inequalities (53) and (54). The numerical minimization has been done using a built-in function in Wolfram Mathematica [67] called *NMinimize* where we specified the used optimization method. On a standard desktop computer, the numerical minimization takes from a few seconds in the case of  $N = 3$  up to 20 seconds in the case of  $N = 6$ . Those times are approximately the same as for criteria in [36] used on the same devices. Our analysis reveals that for all considered values of the squeezing the differences are very small but always strictly positive numbers, which confirms correctness of the proposed criteria.

Next, we demonstrate the ability of the proposed criteria to detect GME. First, we show this on two sets of basic GME Gaussian states, including the CV GHZ-like state. Then, we also present two methods allowing us to find numerical examples of Gaussian states whose GME can be verified by our criteria.

### 5.1.1 Analytical examples

Initially, we apply our criteria to the basic Gaussian states, which are widely used for testing of GME criteria. This includes the family of three-mode CV GHZ-like states with CM (8) and the split squeezed states [68] created by splitting of a single squeezed state on two balanced beam splitters, which possesses the following CM:

$$\gamma^{\text{sss}} = \frac{1}{4} \left[ \begin{pmatrix} a_+ & b_+ & -b_+ \\ b_+ & c_+ & d_+ \\ -b_+ & d_+ & c_+ \end{pmatrix} \oplus \begin{pmatrix} a_- & b_- & -b_- \\ b_- & c_- & d_- \\ -b_- & d_- & c_- \end{pmatrix} \right], \quad (55)$$

where

$$\begin{aligned} a_\pm &= 2(1 + e^{\pm 2r}), & b_\pm &= \sqrt{2}(1 - e^{\pm 2r}), \\ c_\pm &= 3 + e^{\pm 2r}, & d_\pm &= 1 - e^{\pm 2r}. \end{aligned} \quad (56)$$

Again, we minimized the difference  $D_P$ , Eq. (48), over the parameters  $\ell_{ij}^\alpha$ . To speed up the numerical search we further imposed on the parameters the following constraint  $-1 \leq \ell_{ij}^\alpha \leq 1$ . The corresponding minimal differences for the CMs (8) and (55) with squeezing parameters  $r_i = 0.05 \times i$ ,  $i = 0, 1, \dots, 40$  are depicted in Fig. 5. The figure as well as the numerics reveal that for the GHZ-like state except for the case  $r = 0$  for all other considered values of the squeezing the minimized difference is negative. Similarly, in the case of the split squeezed state the minimized difference becomes negative as soon as the considered value of squeezing exceeds the value of  $r = 0.6$ . These two examples clearly demonstrate the ability of the proposed product criterion (53) to detect GME of basic three-mode Gaussian states.

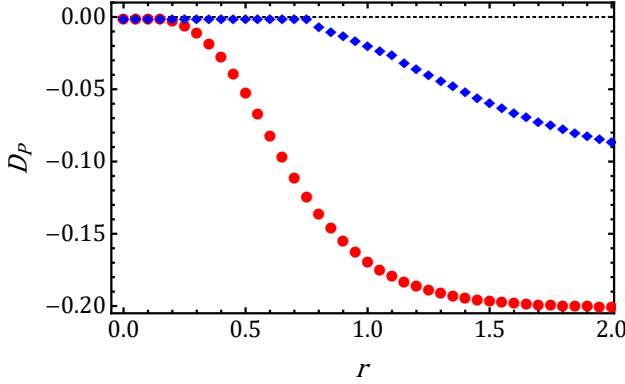


Figure 5: Difference  $D_P$ , Eq. (48), minimized over the elements  $\ell_{ij}^\alpha \in [-1, 1]$  for the CV GHZ-like state with CM (8) (red circles) and the split squeezed state with CM (55) (blue diamonds) versus the squeezing parameter  $r$ . See text for details.

Interestingly, the sum criterion (54) fails to detect GME of any of the previous three-mode states detected by the product criterion. Nevertheless, one can find examples of three-mode GME Gaussian states, which are detected by both criteria or only by the sum criterion itself.

### 5.1.2 Numerical examples

We find examples of Gaussian states whose GME can be detected by the sum criterion (54) using the Gaussian analog [43] of the iterative algorithm [41]. Initially, a pure-state CM  $\gamma^{(0)}$  is randomly generated. In the first step of the algorithm an optimal witness  $Z^{(1)}$  detecting GME from minimal set of two-mode marginal CMs of CM  $\gamma^{(0)}$  is found. The second step consists of finding an optimal CM  $\gamma^{(1)}$  minimizing  $\text{Tr}(\gamma Z^{(1)})$ . In the next iteration the output CM  $\gamma^{(1)}$  is taken as an input to the first step which produces an optimal witness  $Z^{(2)}$ . The new witness is then used in the second step to get optimal CM  $\gamma^{(2)}$  for the witness, etc. By performing few iterations of the algorithm on a randomly generated seed CMs we produced one hundred CMs of GME states, which were

then tested by our product and sum GME criteria (53) and (54). In total, our criteria were capable of detecting GME for nearly 80% of the CMs. One of the obtained CMs is given by

$$\gamma_1 = \begin{pmatrix} 6.3 & -6.6 & 2.8 \\ -6.6 & 10 & -5.6 \\ 2.8 & -5.6 & 5.4 \end{pmatrix} \oplus \begin{pmatrix} 5.4 & 5.3 & 4 \\ 5.3 & 5.5 & 4.2 \\ 4 & 4.2 & 3.5 \end{pmatrix}, \quad (57)$$

where the elements were rounded for brevity to one decimal place in which case physicality of the rounded CM remained preserved. Minimization of the differences  $D_P$  and  $D_S$  over the parameters  $\ell_{ij}^\alpha \in [-1, 1]$  yields  $D_P = -0.245$  and  $D_S = -0.165$ , where the respective rounded optimal values of the parameters  $\ell_{ij}^\alpha$  can be found in Appendix C. As both the differences are negative the GME of the state with CM (57) is detected both by the product criterion (53), as well as sum criterion (54).

Analogously as in the case of CM (57) we can find a CM of a Gaussian state whose GME is detected only by the sum criterion. The CM in question has integer entries and it is of the following form:

$$\gamma_2 = \begin{pmatrix} 5 & -5 & -2 \\ -5 & 7 & 3 \\ -2 & 3 & 2 \end{pmatrix} \oplus \begin{pmatrix} 3 & 4 & -3 \\ 4 & 6 & -5 \\ -3 & -5 & 6 \end{pmatrix}. \quad (58)$$

Indeed, while the product criterion (53) yields a non-negative minimal difference  $D_P$  and thus it does not detect GME, for the sum criterion (54) one gets  $D_S = -0.070$ , which clearly confirms the presence of GME in the considered state. The rounded optimal values of the parameters  $\ell_{ij}^\alpha$  attaining the latter difference are given explicitly in Appendix C.

### 5.1.3 Example derived from a guessed witness

There is yet another method of how one can find examples of three-mode Gaussian states violating inequality (54). What is more, below we use the method to find examples of GME states detected by the sum criteria for more than three modes.

Typically, the inseparability criteria based on uncertainty relations are tailored to the state whose entanglement is to be detect, which is known. Here, on the other hand, we know the criteria and seek states, which are detected by them. This task can be solved relatively easily if we set the parameters  $\ell_{ij}^\alpha$  to suitable values. Namely, by using Eq. (18) and dividing the LHS of the criterion with the RHS, we can express the inequality (46) in the form  $\text{Tr}[\gamma Z] \geq 1$ , where  $Z = Z^x \oplus Z^p$  and  $\gamma = \gamma^x \oplus \gamma^p$ . Here,  $Z$  is a real  $2N \times 2N$  symmetric positive-semidefinite matrix and provided that the parameters  $\ell_{ij}^\alpha$  are chosen properly, it can detect GME. In fact, the matrix  $Z$  is nothing but the already mentioned GME witness in the space of covariance matrices [33].

In order to learn whether the guessed matrix  $Z$  will detect GME, we have to perform its symplectic diag-

onalization. Since typically  $Z > 0$ , there is a symplectic matrix  $S$ , i.e., a real  $2N \times 2N$  matrix satisfying the symplectic condition  $S\Omega_N S^T = \Omega_N$ , which transforms the matrix as [69]

$$SZS^T = \text{diag}(\nu_1, \nu_2, \dots, \nu_N, \nu_1, \nu_2, \dots, \nu_N) \equiv Z_W. \quad (59)$$

Here,  $Z_W$  is a diagonal matrix, where the entries  $\nu_i > 0$ ,  $i = 1, 2, \dots, N$ , are the so-called symplectic eigenvalues. Now, if  $\text{Tr}[Z_W] < 1$  there will be always a CM  $\gamma$ , for which  $\text{Tr}(\gamma Z) < 1$ , which evidences the presence of GME. To see this, note that  $\text{Tr}[Z_W] = \text{Tr}[SZS^T] = \text{Tr}[S^T SZ]$ , so if we set  $\gamma = S^T S$ , we have  $\text{Tr}[\gamma Z] < 1$  and thus the witness matrix  $Z$  detects GME carried by the CM  $\gamma$ .

The GME witness  $Z$  can be obtained, e.g., by setting some parameters  $\ell_{ij}^\alpha$  equal to  $+1$  or  $-1$ , often small parameters, like  $\ell_{33}^\alpha$ , equal to  $10^{-2}$ , and by guessing the remaining free parameters. For example, consider the values of the parameters  $\ell_{ij}^\alpha$  in Tab. 2. Then using Fig. 4 we get  $\mathcal{K}^{(1)} \doteq 86$

Table 2: Guessed values of parameters  $\ell_{ij}^\alpha$ ,  $\alpha = x, p$ , used to get a GME witness  $Z_3$ .

$\ell_{11}^x$	8
$\ell_{21}^x$	-1
$\ell_{22}^x$	1
$\ell_{32}^x$	-1
$\ell_{33}^x$	0.01
$\ell_{11}^p$	10
$\ell_{21}^p$	2
$\ell_{22}^p$	5
$\ell_{32}^p$	1
$\ell_{33}^p$	0.01

and  $\mathcal{K}^{(3)} \doteq 84$ . Hence, the witness matrix  $Z_3 = [L^x(L^x)^T \oplus L^p(L^p)^T]/(2\mathcal{K}^{(3)})$  is

$$Z_3 = \frac{1}{168} \left[ \begin{pmatrix} 64 & -8 & 0 \\ -8 & 2 & -1 \\ 0 & -1 & 1.0001 \end{pmatrix} \right. \\ \left. \oplus \begin{pmatrix} 100 & 20 & 0 \\ 20 & 29 & 5 \\ 0 & 5 & 1.0001 \end{pmatrix} \right]. \quad (60)$$

Next, we find numerically the matrix  $S_3$  symplectically diagonalizing  $Z_3$ , calculate the CM  $\gamma_3 = S_3^T S_3$ , round it for brevity to two decimal places and add to the rounded matrix  $10^{-2} \times \mathbb{1}$  to get a physical CM (see Appendix D.1 for details of the derivation). Thus we arrive at the CM

$$\gamma_3 = \left( \begin{array}{ccc} 1.40 & 1.15 & 0.30 \\ 1.15 & 7.64 & 2.48 \\ 0.30 & 2.48 & 1.49 \end{array} \right) \\ \oplus \left( \begin{array}{ccc} 0.84 & -0.15 & 0.09 \\ -0.15 & 0.33 & -0.50 \\ 0.09 & -0.50 & 1.49 \end{array} \right). \quad (61)$$

To be able to compare the strength of violation of the criterion (46) by CM  $\gamma_3$  with previous examples, we again optimize the difference (49) over  $\ell_{ij}^\alpha \in [-1, 1]$ , which yields  $D_S = -0.15$ . This once again confirms that the proposed sum criterion can really detect GME from minimal set of two-mode marginals.

In the next section we use the latter method to derive Gaussian GME states of  $N = 4, 5$  and  $6$  modes, which are detected by the sum criteria (46) corresponding to different trees.

### 5.1.4 Effect of losses

In the last part of this section, we discuss the effect of imperfections that may occur in the possible experimental preparation of some of the investigated three-mode states on the detection of the given state by the product criterion (53). The imperfection we focus on takes the form of the transition of the states through a lossy channel with intensity transmissivity  $\eta$ . Our analysis starts with the three-mode CV GHZ-like state with CM (8). The best loss robustness for the product criterion (53) is found for squeezing parameter  $r = 0.65$  ( $-5.65$  dB), where minimal transmissivity is approximately  $\eta = 0.96$  or 4% loss. Better resilience to losses can be found in the case of the numerically found state with CM (57) where the minimal transmissivity is around  $\eta = 0.92$  or 8% of losses for the form with elements rounded to one decimal place. The original form of CM (57) is even more robust with minimal transmissivity  $\eta = 0.89$  or 11% of losses. Quadrature squeezing required to prepare the state with the CM (57) is around  $-10$  dB. From the experimental perspective it is desirable to look for states requiring smaller amounts of squeezing for the preparation. In that case, we can find another numerical example of a state with CM given in the Appendix E that requires only  $-4.46$  dB of squeezing. This state can be detected using the presented criteria (53) starting from a minimal transmissivity of the lossy channel  $\eta = 0.90$  or 10% of losses.

## 5.2 Multi-mode states

It remains to clarify whether the proposed criteria are also capable to certify GME in states with more than three modes. Below we use the method of previous section to construct examples of Gaussian states of up to six modes, whose GME is detected by our criteria. As the method is based on the sum criterion (46), the obtained examples violate the sum criterion pronouncedly stronger than the product criterion which often fails to detect the GME of the constructed state. For this reason, the following discussion is restricted to the sum criterion (46).

Initially, we apply the criterion to the four-mode CV GHZ-like state [38]. However, for  $r \in (0, 2]$ , and both configurations 4a and 4b (second and third row of Tab. 3), we did not find any set of parameters  $\ell_{ij}^\alpha$ , for which the sum criterion (46) (as well as the product criterion (43)) would be violated. This indicates that the proposed criteria are not suitable for detection of the GME carried by multi-mode GHZ-like states. This can be attributed to the specific form of GME carried by the GHZ-like states, which manifests itself,

as far as the momentum quadratures is concerned, by squeezing in the global quadrature combination  $\sum_{i=1}^4 p_i$ , whereas the proposed criteria contain only selected two-mode momentum quadrature combinations which are for the studied GHZ-like state contaminated by noise.

Nevertheless, using the method of previous section we found examples of GME states of  $N = 4, 5$  and  $6$  modes detectable by the sum criterion for almost all configurations. The exception being criteria corresponding to the five-mode and six-mode linear tree and the six-mode star tree, for which we so far did not succeed in guessing the GME witness  $Z$ . The best results obtained by us are summarized in Tab. 3. The table contains all non-isomorphic trees with up to six vertices, which are rooted and labelled such that the respective sum criterion contains variances of at most two-mode quadrature combinations. The values of the corresponding difference  $D_S$ , Eq. (49), are for given  $N$  ordered decreasingly. Since optimization over  $\ell_{ij}^\alpha \in [-1, 1]$  yields typically for  $N > 3$  small values of  $D_S$ , the values of the difference in Tab. 3 were obtained for optimization over an extended interval  $\ell_{ij}^\alpha \in [-10, 10]$ . This is why the value of  $D_S$  for the three-mode case is roughly hundred-times larger compared to the examples presented in previous section. The Tab. 3 indicates that up to the configurations 3 and 4a the value of  $D_S$  decreases with increasing  $N$ , which is a typical behaviour of GME states (cf. Tab. I of Ref. [41]). The exception is likely to be attributed to the fact that in the case 3 we guessed a little worse witness than for configuration 4a. All the guessed witnesses, the CMs of the states, and other details of derivation of the results in Tab. 3 are given explicitly in Appendix D.

We accomplished the present analysis by an independent check of the presence of GME verifiable only from the minimal set of two-mode marginal CMs in the Gaussian states used in Tab. 3. For this purpose, we used the already mentioned method of entanglement witnesses in the space of CMs [33], which detect the GME from the minimal set of two-mode marginal CMs [43]. More precisely, for each CM and all considered configurations we found numerically such a witness, which independently confirms the presence of the GME detectable only from the respective minimal set of marginals in the constructed examples.

## 6 Conclusions

In this paper we derived a set of product and sum criteria for GME of continuous-variable systems. The criteria are based on the second moments of quadrature operators and unlike the overwhelming majority of the known GME criteria contain only the variances of at most two-mode quadrature combinations. Moreover, the presented criteria are also minimal in the sense that they contain only the minimum number

Table 3: All non-isomorphic trees with  $N = 3, 4, 5$  and  $6$  vertices. The root of the tree is depicted by a red circle. The linear trees are labeled according to the standard labeling, whereas the other trees are covered by the reverse level order labeling, which lead to the GME criteria involving variances of at most two-mode quadrature combinations. The last column contains the difference  $D_S$ , Eq. (49), for the displayed trees and CMs constructed by means of the method of Subsec. 5.1.3. The values of  $D_S$  are calculated for the values of parameters  $\ell_{ij}^\alpha$  found by a numerical minimization over  $\ell_{ij}^\alpha \in [-10, 10]$ . The cases for which we did not find an example are denoted by a cross. Explicit form of all the CMs as well as other details of derivation of  $D_S$  can be found in Appendix D. See text for details.

$N$	Index	Labelled tree	Difference $D_S$
3	3	(1)–(2)–(3)	-17.87
4	4a	(1)–(2)–(3)–(4)	-20.31
	4b	(3)–(4)–(1) (2)	-5.36
5	5a	(1)–(2)–(3)–(4)–(5)	×
	5b	(1) (4)–(5)–(2) (3)	-3.64
	5c	(1)–(2)–(5)–(4) (3)	-2.30
6	6a	(1)–(2)–(3)–(4)–(5)–(6)	×
	6b	(1)–(2) (5)–(6)–(3) (4)	×
	6c	(2)–(5)–(6)–(3)–(1) (4)	-1.00
	6d	(3)–(5)–(6)–(4)–(1) (2)	-0.91
	6e	(2)–(5)–(6)–(3) (1)–(5) (4)	-0.65
	6f	(5)–(6)–(4)–(2) (3)	-0.13

of the latter variances. In other words, the criteria require only the knowledge of the minimal set of two-mode marginal CMs, which consists of  $7N - 4$  independent CM elements of the state under study [43]. Since our criteria do not take into account the  $x - p$  correlations, the number of the elements further reduces to  $4N - 2$  and thus it scales only linearly with the number of modes. This distinguishes our criteria from the most commonly used GME criteria [36–38], which require knowledge of the entire CM without

$x - p$  correlations, i.e., knowledge of its  $N(N + 1)$  elements. Other known  $N$ -mode CV GME criteria [33] utilize the whole CM including  $x - p$  correlations, i.e., to use them one needs to know its  $N(2N + 1)$  elements. All these criteria thus scale quadratically with the number of modes. Since any minimal set of marginal CMs can be represented by a special kind of a graph known as a tree, each criterion is intimately associated to a particular tree. This allowed us to develop a method of construction of all the sum criteria directly from the underlying tree.

Further, we have shown that the product criterion detects GME of the three-mode CV GHZ-like state and the split squeezed state, but neither of the states is detected by the sum criterion. The fact that we detected GME in the three-mode CV GHZ-like state from its two-mode marginals is in contrast with results for qubit GHZ state where this is not possible [44]. We have also constructed numerical examples of three-mode Gaussian GME states which are simultaneously detected by both the criteria as well as only by the sum criterion. To get examples of GME states detected by our criteria for more than three modes, we developed a method based on symplectic diagonalization of a guessed witness in the space of CMs. Thus we found states detected by the sum criterion for nearly all configurations of up to six modes.

Interestingly, our criteria do not detect the GME in three- and four-mode GME states with all two-mode marginals separable, which were recently found in Ref. [43]. Therefore, we tested the criteria for another more than hundred numerically generated GME states with separable marginals and we always got a negative result. This rises a question of how to modify the present criteria so as to make them capable of detecting the GME from separable marginals, which is deferred for further research. Likewise, inspired by the existence of the CV GME criteria for higher-order moments [70, 71] we could try to generalize the proposed criteria to the higher-order moments, which is thus another open problem. Finally, one may ask whether the present algorithm can be used to derive analogous minimal criteria for genuine multipartite quantum steering [68, 72]. Since the steering criteria are typically obtained only by small modifications of derivation of the standard GME criteria [27, 36], we expect that the same approach will be viable also in the case of our criteria, which will be addressed elsewhere.

The present paper provides a rigorous method of construction of minimal criteria of GME. The method relies on the concept of witness matrix in the space of CMs and graph theory, and gives a recipe of how to systematically construct similar minimal criteria for other types of multipartite quantum correlations. The GME criteria presented here are also experimentally friendly as they are simple and immediately reveal how to measure them. What is more, the criteria do

not require to measure entire CM but only its strictly smaller part which is needed for detection of GME. This feature provides an advantage compared to other GME criteria by saving the number of measurements needed for testing of GME of the investigated state. We believe that our results will stimulate theoretical research of minimal criteria of multipartite quantum properties and find applications in characterization of the properties in experimentally prepared quantum states.

## Acknowledgments

O.L. acknowledges support from IGA-PrF-2023-006 and the European Union's 2020 research and innovation program (CSA - Coordination and support action, H2020-WIDESPREAD-2020-5) under grant agreement No. 951737 (NONGAUSS). O.L. and L.M. acknowledge the project 8C22002 (CVStar) of MEYS of the Czech Republic, which has received funding from the European Union's Horizon 2020 research and innovation programme under the Grant Agreements no. 731473 and 10101773; and the project 'Quantum Secure Networks Partnership' (QSNP), which has received funding from the European Union's Horizon Europe research and innovation programme under the Grant Agreement no. 101114043.

## Author contribution

Both authors contributed equally to the results and the manuscript writing.

## A Fully inseparable biseparable Gaussian state

This section is dedicated to the proof that the three-mode biseparable state (11) with CM (12) is in a certain region of squeezing parameters fully inseparable, i.e., it is entangled across all three bipartite splits  $1|23$ ,  $2|31$  and  $3|12$ . The state possesses a fully symmetric CM of the form

$$\gamma^{\text{test}} = \begin{pmatrix} b & e & e \\ e & b & e \\ e & e & b \end{pmatrix} \oplus \begin{pmatrix} b & -e & -e \\ -e & b & -e \\ -e & -e & b \end{pmatrix}, \quad (62)$$

where

$$b = \frac{2 \cosh(2r) + 1}{3}, \quad e = \frac{\sinh(2r)}{3}. \quad (63)$$

Due to the symmetry it is sufficient to verify entanglement of the state with respect to just one split, e.g.,  $3|12$ , which we will do using the results of Ref. [73, 74]. Interference of modes 1 and 2 on a balanced beam splitter does not change entanglement

properties across the split and decouples mode 2 from modes 1 and 3. Hence, we are left with the CM

$$\gamma_{13}^{\text{test}} = \begin{pmatrix} b+e & \sqrt{2}e \\ \sqrt{2}e & b \end{pmatrix} \oplus \begin{pmatrix} b-e & -\sqrt{2}e \\ -\sqrt{2}e & b \end{pmatrix} \quad (64)$$

of modes 1 and 3. Entanglement of the state with the latter CM then can be proved easily by using positive partial transposition criterion [54] expressed in terms of the symplectic eigenvalues [74]. The partial transposition operation with respect to mode 3 transforms the CM (64) as  $\gamma_{13}^{\text{test}(T_3)} = (\mathbb{1} \oplus \sigma_z)\gamma_{13}^{\text{test}}(\mathbb{1} \oplus \sigma_z)$  and its symplectic eigenvalues  $\mu_{\pm}$  are obtained from the spectrum  $\{\pm i\mu_+, \pm i\mu_-\}$  of the matrix  $\Omega_2\gamma_{13}^{\text{test}(T_3)}$  [74] in the form

$$\mu_{\pm} = \sqrt{\frac{\alpha \pm \sqrt{\alpha^2 - 4\beta}}{2}}, \quad (65)$$

where  $\alpha = 2b^2 + 3e^2$  and  $\beta = (b^2 - 2e^2)^2 - (be)^2$ . According to the partial transposition criterion the state with CM (64) is entangled if the minimal symplectic eigenvalue  $\mu_-$  satisfies  $\mu_- < 1$ . Thus we are looking for an interval of squeezing parameters  $r \geq 0$ , for which  $\mu_- < 1$ . In Fig. 6 we plot the dependence of the symplectic eigenvalue  $\mu_-$  on the squeezing parameter  $r$ . The figure shows that as  $r$  increases from

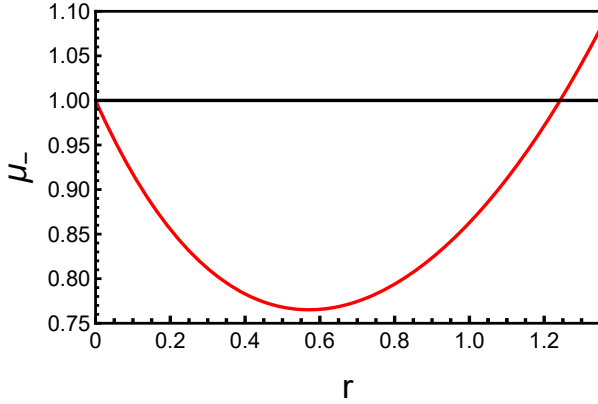


Figure 6: Lower symplectic eigenvalue  $\mu_-$ , Eq. (65), versus the squeezing parameter  $r$  for the state with CM  $\gamma_{13}^{\text{test}}$ , Eq. (64).

$r = 0$  when  $\mu_- = 1$  the symplectic eigenvalue satisfies  $\mu_- < 1$  for up to  $r = r_{\max}$  when  $\mu_- = 1$  and then  $\mu_- > 1$  with further increase of  $r$ . The threshold value of  $r_{\max}$  can be calculated from the condition  $\mu_- = 1$ , which simplifies to  $\alpha - \beta = 1$  and leads further to the following equation:

$$3e^{12r} - 34e^{10r} - 35e^{8r} + 132e^{6r} - 35e^{4r} - 34e^{2r} + 3 = 0. \quad (66)$$

Upon solving the latter equation numerically one finally finds  $r_{\max} \doteq 1.24$  and thus the state with CM (64) is entangled for  $r \in (0, 1.24)$ . As a consequence, the state with CM (62) is fully inseparable for  $r \in (0, 1.24)$ .

## B Derivation of the structure of the matrix $Z_A^{\alpha}$ providing two-mode quadrature combinations $u_i^{\alpha}$

In this section we show what structure the matrix  $Z_A^{\alpha}$  must have for the operators  $u_i^{x,p}$ ,  $i = 1, 2, \dots, N-1$ , Eq. (19) of the main text, to contain at most two non-zero terms. In the main text, we showed that for operators  $u_i^{x,p}$  to contain at most two non-zero terms, the vectors  $L_{i+1:N,i}^{\alpha}$ ,  $i = 1, 2, \dots, N-1$ , Eq. (23) of the main text, have to possess at most one non-zero component. Below we show that the vectors  $L_{i+1:N,i}^{\alpha}$ , will have at most one non-zero component if the vectors  $(Z_A^{\alpha})_{i+1:N,i}$ ,  $i = 1, 2, \dots, N-1$ , contain at most one non-zero component.

Namely, for a positive-definite matrix  $Z_A^{\alpha}$  the vectors  $L_{i+1:N,i}^{\alpha}$  can be expressed as [63, Theorem 4.2.5]

$$L_{2:N,1}^{\alpha} = \frac{(Z_A^{\alpha})_{2:N,1}}{L_{11}^{\alpha}} \quad (67)$$

and

$$L_{i+1:N,i}^{\alpha} = \frac{1}{L_{ii}^{\alpha}} \left[ (Z_A^{\alpha})_{i+1:N,i} - \sum_{j=1}^{i-1} L_{ij}^{\alpha} L_{i+1:N,j}^{\alpha} \right] \quad (68)$$

for  $i = 2, 3, \dots, N-1$ . From Eq. (67) it then follows that the vector  $L_{2:N,1}^{\alpha}$  will contain at most one non-zero component if the vector  $(Z_A^{\alpha})_{2:N,1}$  has at most one non-zero component. Moving to the vector  $L_{3:N,2}^{\alpha}$ , Eq. (68) with  $i = 2$ , we see that if the vector  $(Z_A^{\alpha})_{2:N,1}$  has at most one non-zero component, then the second term in the square brackets vanishes because it contains products of different components of the vector  $(Z_A^{\alpha})_{2:N,1}$ , and  $L_{3:N,2}^{\alpha} = (Z_A^{\alpha})_{3:N,2}/L_{22}^{\alpha}$  according to Eq. (68). Again, in order the vector  $L_{3:N,2}^{\alpha}$  to have at most one non-zero component, the vector  $(Z_A^{\alpha})_{3:N,2}$  has to possess at most one non-zero component. Repeating the same procedure  $(i-1)$ -times we see that the vectors  $L_{j+1:N,j}^{\alpha}$ ,  $j = 1, 2, \dots, i-1$  will have at most one non-zero component if the same holds for vectors  $(Z_A^{\alpha})_{j+1:N,j}$ ,  $j = 1, 2, \dots, i-1$ . If this is the case, then the sum  $\sum_{j=1}^{i-1} L_{ij}^{\alpha} L_{i+1:N,j}^{\alpha}$  in Eq. (68) vanishes, because each term  $L_{ij}^{\alpha} L_{i+1:N,j}^{\alpha}$  is a vector with components given by a product of *different* components of the vector  $(Z_A^{\alpha})_{j+1:N,j}$ . The  $i$ -th vector (68) of the Cholesky matrix  $L^{\alpha}$  then reduces to

$$L_{i+1:N,i}^{\alpha} = \frac{(Z_A^{\alpha})_{i+1:N,i}}{L_{ii}^{\alpha}} \quad (69)$$

and again it has at most one non-zero component if the vector  $(Z_A^{\alpha})_{i+1:N,i}$  contains at most one non-zero component.

Summarizing the obtained results we see that if we require all the quadrature combinations  $u_i^{x,p}$ , Eq. (19) of the main text, to contain at most two non-zero terms, then all vectors  $(Z_A^{\alpha})_{i+1:N,i}$ ,  $i = 1, 2, \dots, N-1$

have to possess at most one non-zero component, as we wanted to prove.

## C Optimal parameters

This section contains optimal values of the parameters  $\ell_{ij}^\alpha$  minimizing the differences (48) and (49) between the LHS and the RHS of the proposed minimal GME criteria.

For the three-mode CM (57) and the product criterion (53) the optimal parameters  $\ell_{ij}^\alpha$  are summarized in Tab. 4

Table 4: Rounded values of the parameters  $\ell_{ij}^\alpha \in [-1, 1]$ ,  $\alpha = x, p$ , used to calculate the difference  $D_P = -0.245$  for the product criterion (53) and the CM  $\gamma_1$ , Eq. (57).

$\ell_{11}^x$	0.947
$\ell_{21}^x$	0.760
$\ell_{22}^x$	0.860
$\ell_{32}^x$	1
$\ell_{33}^x$	$1 \times 10^{-5}$

$\ell_{11}^p$	0.989
$\ell_{21}^p$	-0.987
$\ell_{22}^p$	0.817
$\ell_{32}^p$	-1
$\ell_{33}^p$	$1.8 \times 10^{-6}$

In the case of CM (57) and the sum criterion (54) the optimal parameters  $\ell_{ij}^\alpha$  are summarized in Tab. 5

Table 5: Rounded values of the parameters  $\ell_{ij}^\alpha \in [-1, 1]$ ,  $\alpha = x, p$ , used to calculate the difference  $D_S = -0.165$  for the sum criterion (54) and the CM  $\gamma_1$ , Eq. (57).

$\ell_{11}^x$	0.425
$\ell_{21}^x$	0.253
$\ell_{22}^x$	0.305
$\ell_{32}^x$	0.505
$\ell_{33}^x$	$2 \times 10^{-4}$

$\ell_{11}^p$	1
$\ell_{21}^p$	-0.954
$\ell_{22}^p$	0.792
$\ell_{32}^p$	-1
$\ell_{33}^p$	$4 \times 10^{-4}$

Optimal parameters  $\ell_{ij}^\alpha$  for the CM (58) and the sum criterion (54) are summarized in Tab. 6

$$\gamma'_3 = S_3^T S_3 = \begin{pmatrix} 1.38922 & 1.14998 & 0.299419 \\ 1.14998 & 7.63236 & 2.48042 \\ 0.299419 & 2.48042 & 1.48411 \end{pmatrix} \oplus \begin{pmatrix} 0.827955 & -0.15424 & 0.0907433 \\ -0.15424 & 0.315532 & -0.49624 \\ 0.0907433 & -0.49624 & 1.48488 \end{pmatrix}. \quad (73)$$

Next, for simplicity we round all elements of the latter CM to two decimal places thereby getting the matrix  $\bar{\gamma}_3$ , which slightly violates the Heisenberg uncertainty principle  $\gamma + i\Omega_3 \geq 0$  [54], Eq. (6) with  $N = 3$  of the main text. Therefore, we have added to the CM a small amount of thermal noise thereby creating a physical CM  $\gamma_3 = \bar{\gamma}_3 + 0.01 \times \mathbb{1}$  given explicitly in Eq. (61). Now, if we optimize numerically the difference (49) for the sum criterion (54) over the parameters  $\ell_{ij}^\alpha \in [-1, 1]$ , we arrive at  $D_S = -0.15$  and the

Table 6: Rounded values of the parameters  $\ell_{ij}^\alpha \in [-1, 1]$ ,  $\alpha = x, p$ , used to calculate the difference  $D_S = -0.070$  for the sum criterion (54) and the CM  $\gamma_2$ , Eq. (58).

$\ell_{11}^x$	0.514
$\ell_{21}^x$	0.314
$\ell_{22}^x$	0.419
$\ell_{32}^x$	-0.908
$\ell_{33}^x$	$3 \times 10^{-5}$
$\ell_{11}^p$	1
$\ell_{21}^p$	-0.652
$\ell_{22}^p$	0.489
$\ell_{32}^p$	0.559
$\ell_{33}^p$	$8.7 \times 10^{-7}$

## D Derivation of examples from a guessed witness

In this section we present a complete derivation of Gaussian states of  $N \geq 3$  modes violating minimal GME criteria (43) and (46), based on a guessed witness in the space of CMs.

### D.1 N=3

We start with the guessed three-mode witness matrix  $Z_3$ , Eq. (60). Making use of the method [75], we can find numerically the matrix  $S_3$  symplectically diagonalizing  $Z_3$  in the form

$$S_3 = \begin{pmatrix} \mathbb{0}_3 & X_3 \\ Y_3 & \mathbb{0}_3 \end{pmatrix}, \quad (70)$$

where

$$X_3 = \begin{pmatrix} -0.0445813 & 0.222904 & -1.11455 \\ 0.0879785 & -0.503613 & 0.492602 \\ 0.904559 & -0.110546 & -0.00252406 \end{pmatrix} \quad (71)$$

and

$$Y_3 = \begin{pmatrix} -0.139315 & -1.11452 & -1.11455 \\ -0.309427 & -2.52072 & -0.491755 \\ 1.12874 & 0.190238 & -0.00710211 \end{pmatrix}. \quad (72)$$

From the symplectic matrix (70) we then get the following CM:

optimal parameters are listed in Tab. 7.

Table 7: Rounded values of the parameters  $\ell_{ij}^\alpha \in [-1, 1]$ ,  $\alpha = x, p$ , used to calculate the difference (49) for the sum criterion (54) and the CM  $\gamma_3$ , Eq. (61).

$\ell_{11}^x$	0.90
$\ell_{21}^x$	-0.23
$\ell_{22}^x$	0.23
$\ell_{32}^x$	-1
$\ell_{33}^x$	0.01
$\ell_{11}^p$	1
$\ell_{21}^p$	0.98
$\ell_{22}^p$	1
$\ell_{32}^p$	1
$\ell_{33}^p$	0.01

The difference (49) in the first row of Tab. 3 of the main text has been calculated for the unrounded CM  $\gamma'_3$ , Eq. (73). If we optimize numerically the difference (49) for the sum criterion (54) over the parameters  $\ell_{ij}^\alpha \in [-10, 10]$ , we arrive at  $D_S = -17.87$  and the optimal parameters are listed in Tab. 8.

Table 8: Rounded values of the parameters  $\ell_{ij}^\alpha \in [-10, 10]$ ,  $\alpha = x, p$ , used to calculate the difference  $D_S$ , Eq. (49), given in the first row of Tab. 3 for the CM  $\gamma'_3$ , Eq. (73).

$\ell_{11}^x$	9.11
$\ell_{21}^x$	-2.31
$\ell_{22}^x$	2.31
$\ell_{32}^x$	-10
$\ell_{33}^x$	0.01
$\ell_{11}^p$	10
$\ell_{21}^p$	10
$\ell_{22}^p$	10
$\ell_{32}^p$	10
$\ell_{33}^p$	0.01

## D.2 N=4

### D.2.1 Linear tree 4a

We start with the guessed four-mode witness matrix  $Z_{4a}$  of the linear tree 4a,

$$Z_{4a} = \frac{1}{5.5002} \begin{pmatrix} Z_{4a}^x & \mathbb{0}_4 \\ \mathbb{0}_4 & Z_{4a}^p \end{pmatrix}, \quad (74)$$

where

$$Z_{4a}^x = \begin{pmatrix} 1 & -0.5 & 0 & 0 \\ -0.5 & 0.5 & -0.5 & 0 \\ 0 & -0.5 & 1.25 & -0.5 \\ 0 & 0 & -0.5 & 1.0001 \end{pmatrix}$$

and

$$Z_{4a}^p = \begin{pmatrix} 1 & 0.5 & 0 & 0 \\ 0.5 & 0.5 & 0.5 & 0 \\ 0 & 0.5 & 1.25 & 0.5 \\ 0 & 0 & 0.5 & 1.0001 \end{pmatrix}.$$

Next, we find numerically the matrix  $S_{4a}$  symplectically diagonalizing  $Z_{4a}$  in the form:

$$S_{4a} = \begin{pmatrix} \mathbb{0}_4 & X_{4a} \\ Y_{4a} & \mathbb{0}_4 \end{pmatrix}, \quad (75)$$

where

$$X_{4a} = \begin{pmatrix} -0.666646 & 1.33331 & -0.666635 & 0.333288 \\ -1.05853 & 0.895417 & -0.870291 & 0.275906 \\ 0.0468749 & -0.178567 & -0.191418 & 1.00347 \\ 0.571074 & 0.0886146 & -0.850668 & 0.204715 \end{pmatrix} \quad (76)$$

and

$$Y_{4a} = \begin{pmatrix} -0.666646 & -1.33331 & -0.666635 & -0.333288 \\ 1.05853 & 0.895417 & 0.870291 & 0.275906 \\ 0.0468749 & 0.178567 & -0.191418 & -1.00347 \\ -0.571074 & 0.0886146 & 0.850668 & 0.204715 \end{pmatrix}. \quad (77)$$

From the symplectic matrix (75) we then get the following CM:

$$\gamma_{4a} = S_{4a}^T S_{4a} = \begin{pmatrix} 1.89322 & 1.79444 & 0.87087 & 0.350295 \\ 1.79444 & 2.61924 & 1.70931 & 0.530383 \\ 0.87087 & 1.70931 & 1.96209 & 0.828527 \\ 0.350295 & 0.530383 & 0.828527 & 1.23606 \end{pmatrix} \oplus \begin{pmatrix} 1.89322 & -1.79444 & 0.87087 & -0.350295 \\ -1.79444 & 2.61924 & -1.70931 & 0.530383 \\ 0.87087 & -1.70931 & 1.96209 & -0.828527 \\ -0.350295 & 0.530383 & -0.828527 & 1.23606 \end{pmatrix}. \quad (78)$$

Now, if we optimize numerically the difference (49) for the sum criterion (46) over the parameters  $\ell_{ij}^\alpha \in [-10, 10]$ , we arrive at  $D_S = -20.31$  and the optimal parameters are listed in Tab. 9.

### D.2.2 Star tree 4b

We guess the four-mode witness matrix  $Z_{4b}$  corresponding to the star tree 4b in the following form:

$$Z_{4b} = \frac{1}{68.02} \begin{pmatrix} Z_{4b}^x & \mathbb{0}_4 \\ \mathbb{0}_4 & Z_{4b}^p \end{pmatrix}, \quad (79)$$

Table 9: Rounded values of the parameters  $\ell_{ij}^\alpha \in [-10, 10]$ ,  $\alpha = x, p$ , used to calculate the difference (49) for the sum criterion (46) and the CM  $\gamma_{4a}$ , Eq. (78).

$\ell_{11}^x$	10
$\ell_{21}^x$	-5.08
$\ell_{22}^x$	5.09
$\ell_{32}^x$	-9.03
$\ell_{33}^x$	5.07
$\ell_{43}^x$	-10
$\ell_{44}^x$	0.01
$\ell_{11}^p$	10
$\ell_{21}^p$	5.08
$\ell_{22}^p$	5.08
$\ell_{32}^p$	-9.03
$\ell_{33}^p$	5.10
$\ell_{43}^p$	10
$\ell_{44}^p$	0.01

where

$$Z_{4b}^x = \begin{pmatrix} 4 & 0 & 0 & -2 \\ 0 & 1 & 0 & -1 \\ 0 & 0 & 4 & -2 \\ -2 & -1 & -2 & 3.01 \end{pmatrix}$$

and

$$Z_{4b}^p = \begin{pmatrix} 100 & 0 & 0 & 10 \\ 0 & 25 & 0 & 5 \\ 0 & 0 & 25 & 5 \\ 10 & 5 & 5 & 3.01 \end{pmatrix}.$$

The matrix  $S_{4b}$  symplectically diagonalizing  $Z_{4b}$  is of the form:

$$S_{4b} = \begin{pmatrix} V_{4b} & X_{4b} \\ Y_{4b} & W_{4b} \end{pmatrix}, \quad (80)$$

where

$$V_{4b} = \begin{pmatrix} 0 & 0 & 0 & 0 \\ 0 & 0 & 0 & 0 \\ 0.258041 & -0.339431 & 1.61423 & 0.280456 \\ 0 & 0 & 0 & 0 \end{pmatrix}, \quad (81)$$

$$X_{4b} = \begin{pmatrix} -0.123786 & -0.247003 & -0.247382 & 1.23881 \\ -0.0795257 & -0.506179 & -0.206184 & 0.647292 \\ 0 & 0 & 0 & 0 \\ 0.454241 & -0.0135947 & -0.0420425 & -0.192404 \end{pmatrix}, \quad (82)$$

$$Y_{4b} = \begin{pmatrix} 0.61893 & 1.23502 & 0.618456 & 1.23881 \\ -0.397629 & -2.53089 & -0.515461 & -0.647292 \\ 0 & 0 & 0 & 0 \\ 2.27121 & -0.0679731 & -0.105106 & 0.192405 \end{pmatrix}, \quad (83)$$

and

$$W_{4b} = \begin{pmatrix} 0 & 0 & 0 & 0 \\ 0 & 0 & 0 & 0 \\ 0.051608 & -0.067886 & 0.645693 & -0.280457 \\ 0 & 0 & 0 & 0 \end{pmatrix}. \quad (84)$$

From the symplectic matrix (80) we then get the following CM:

$$\gamma_{4b} = S_{4b}^T S_{4b} = \begin{pmatrix} 5.76616 & 1.52878 & 0.765563 & 1.53348 \\ 1.52878 & 8.05052 & 1.5276 & 3.0599 \\ 0.765563 & 1.5276 & 3.26498 & 1.5323 \\ 1.53348 & 3.0599 & 1.5323 & 2.06932 \end{pmatrix} \oplus \begin{pmatrix} 0.230645 & 0.061151 & 0.0612449 & -0.306695 \\ 0.061151 & 0.322021 & 0.122208 & -0.611981 \\ 0.0612449 & 0.122208 & 0.522397 & -0.612921 \\ -0.306695 & -0.611981 & -0.612921 & 2.06932 \end{pmatrix}. \quad (85)$$

Now, if we optimize numerically the difference (49) for the sum criterion (46) over the parameters  $\ell_{ij}^\alpha \in [-10, 10]$ , we arrive at  $D_S = -5.36$  and the optimal parameters are listed in Tab. 9.

### D.3 N=5

#### D.3.1 Star tree 5b

We guess the five-mode witness matrix  $Z_{5b}$  corresponding to the star tree 5b,

Table 10: Rounded values of the parameters  $\ell_{ij}^\alpha \in [-10, 10]$ ,  $\alpha = x, p$ , used to calculate the difference (49) for the sum criterion (46) and the CM  $\gamma_{4b}$ , Eq. (85).

$\ell_{11}^x$	2.35	$\ell_{11}^p$	10
$\ell_{41}^x$	-2.27	$\ell_{41}^p$	2.13
$\ell_{22}^x$	2.17	$\ell_{22}^p$	10
$\ell_{42}^x$	-2.42	$\ell_{42}^p$	2.00
$\ell_{33}^x$	4.09	$\ell_{33}^p$	9.99
$\ell_{43}^x$	-2.28	$\ell_{43}^p$	2.13
$\ell_{44}^x$	0.12	$\ell_{44}^p$	0.09

where

$$Z_{5b}^x = \begin{pmatrix} 1 & 0 & 0 & 0 & -0.1 \\ 0 & 0.25 & 0 & 0 & -0.05 \\ 0 & 0 & 1 & 0 & -0.1 \\ 0 & 0 & 0 & 0.25 & -0.05 \\ -0.1 & -0.05 & -0.1 & -0.05 & 0.0401 \end{pmatrix}$$

and

$$Z_{5b}^p = \begin{pmatrix} 1 & 0 & 0 & 0 & 0.1 \\ 0 & 0.25 & 0 & 0 & 0.05 \\ 0 & 0 & 1 & 0 & 0.1 \\ 0 & 0 & 0 & 0.25 & 0.05 \\ 0.1 & 0.05 & 0.1 & 0.05 & 0.0401 \end{pmatrix}.$$

By finding numerically the matrix  $S_{5b}$  symplectically diagonalizing  $Z_{5b}$ , we then get the following CM:

$$\gamma_{5b} = S_{5b}^T S_{5b} = \begin{pmatrix} \gamma_{5b}^x & \mathbb{0}_5 \\ \mathbb{0}_5 & \gamma_{5b}^p \end{pmatrix}, \quad (87)$$

$$Z_{5b} = \frac{1}{2.4801} \begin{pmatrix} Z_{5b}^x & \mathbb{0}_5 \\ \mathbb{0}_5 & Z_{5b}^p \end{pmatrix}, \quad (86)$$

where

$$\gamma_{5b}^x = \begin{pmatrix} 1.02221 & 0.0444158 & 0.0222153 & 0.0444158 & 0.222178 \\ 0.0444158 & 1.0888 & 0.0444158 & 0.0888027 & 0.444208 \\ 0.0222153 & 0.0444158 & 1.02221 & 0.0444158 & 0.222178 \\ 0.0444158 & 0.0888027 & 0.0444158 & 1.0888 & 0.444208 \\ 0.222178 & 0.444208 & 0.222178 & 0.444208 & 1.22203 \end{pmatrix}, \quad (88)$$

$$\gamma_{5b}^p = \begin{pmatrix} 1.02221 & 0.0444158 & 0.0222153 & 0.0444158 & -0.222178 \\ 0.0444158 & 1.0888 & 0.0444158 & 0.0888027 & -0.444208 \\ 0.0222153 & 0.0444158 & 1.02221 & 0.0444158 & -0.222178 \\ 0.0444158 & 0.0888027 & 0.0444158 & 1.0888 & -0.444208 \\ -0.222178 & -0.444208 & -0.222178 & -0.444208 & 1.22203 \end{pmatrix}. \quad (89)$$

Now, if we optimize numerically the difference (49) for the sum criterion (46) over the parameters  $\ell_{ij}^\alpha \in [-10, 10]$ , we arrive at  $D_S = -3.64$ .

### D.3.2 Tree 5c

We start with the guessed five-mode witness matrix  $Z_{5c}$  corresponding to the tree 5c,

$$Z_{5c} = \frac{1}{2.4801} \begin{pmatrix} Z_{5c}^x & \mathbb{0}_5 \\ \mathbb{0}_5 & Z_{5c}^p \end{pmatrix}, \quad (90)$$

where

$$Z_{5c}^x = \begin{pmatrix} 1 & -0.1 & 0 & 0 & 0 \\ -0.1 & 0.26 & 0 & 0 & -0.05 \\ 0 & 0 & 1 & 0 & -0.1 \\ 0 & 0 & 0 & 0.25 & -0.05 \\ 0 & -0.05 & -0.1 & -0.05 & 0.0301 \end{pmatrix}$$

and

$$Z_{5c}^p = \begin{pmatrix} 1 & 0.1 & 0 & 0 & 0 \\ 0.1 & 0.26 & 0 & 0 & 0.05 \\ 0 & 0 & 1 & 0 & 0.1 \\ 0 & 0 & 0 & 0.25 & 0.05 \\ 0 & 0.05 & 0.1 & 0.05 & 0.0301 \end{pmatrix}.$$

Next, we find numerically the matrix  $S_{5c}$  symplectically diagonalizing  $Z_{5c}$  and from that symplectic matrix we then get the following CM:

$$\gamma_{5c} = S_{5c}^T S_{5c} = \begin{pmatrix} \gamma_{5c}^x & \mathbb{0}_5 \\ \mathbb{0}_5 & \gamma_{5c}^p \end{pmatrix}, \quad (91)$$

where

$$\gamma_{5c}^x = \begin{pmatrix} 1.01364 & 0.16921 & 0.00397589 & 0.00844686 & 0.035641 \\ 0.16921 & 1.10058 & 0.0438767 & 0.0877648 & 0.438485 \\ 0.00397589 & 0.0438767 & 1.02196 & 0.0439097 & 0.219645 \\ 0.00844686 & 0.0877648 & 0.0439097 & 1.08779 & 0.439145 \\ 0.035641 & 0.438485 & 0.219645 & 0.439145 & 1.19671 \end{pmatrix}, \quad (92)$$

$$\gamma_{5c}^p = \begin{pmatrix} 1.01364 & -0.16921 & -0.00397589 & -0.00844686 & 0.035641 \\ -0.16921 & 1.10058 & 0.0438767 & 0.0877648 & -0.438485 \\ -0.00397589 & 0.0438767 & 1.02196 & 0.0439097 & -0.219645 \\ -0.00844686 & 0.0877648 & 0.0439097 & 1.08779 & -0.439145 \\ 0.035641 & -0.438485 & -0.219645 & -0.439145 & 1.19671 \end{pmatrix}. \quad (93)$$

Now, if we optimize numerically the difference (49) for the sum criterion (46) over the parameters  $\ell_{ij}^\alpha \in [-10, 10]$ , we arrive at  $D_S = -2.30$ . where

## D.4 N=6

### D.4.1 Tree 6c

The guessed six-mode witness matrix  $Z_{6c}$  for the tree 6c is of the form:

$$Z_{6c} = \frac{1}{3.2301} \begin{pmatrix} Z_{6c}^x & \mathbb{0}_6 \\ \mathbb{0}_6 & Z_{6c}^p \end{pmatrix}, \quad (94)$$

$$Z_{6c}^x = \begin{pmatrix} 1 & 0 & -0.1 & 0 & 0 & 0 \\ 0 & 1 & 0 & 0 & -0.1 & 0 \\ -0.1 & 0 & 1.01 & 0 & 0 & -0.1 \\ 0 & 0 & 0 & 0.25 & 0 & -0.05 \\ 0 & -0.1 & 0 & 0 & 0.02 & -0.01 \\ 0 & 0 & -0.1 & -0.05 & -0.01 & 0.0301 \end{pmatrix}$$

and

$$Z_{6c}^p = \begin{pmatrix} 1 & 0 & 0.1 & 0 & 0 & 0 \\ 0 & 1 & 0 & 0 & 0.1 & 0 \\ 0.1 & 0 & 1.01 & 0 & 0 & 0.1 \\ 0 & 0 & 0 & 0.25 & 0 & 0.05 \\ 0 & 0.1 & 0 & 0 & 0.02 & 0.01 \\ 0 & 0 & 0.1 & 0.05 & 0.01 & 0.0301 \end{pmatrix}.$$

From the numerically calculated matrix  $S_{6c}$  symplectically diagonalizing  $Z_{6c}$  we then get the following where

$$\gamma_{6c} = S_{6c}^T S_{6c} = \begin{pmatrix} \gamma_{6c}^x & \mathbb{0}_6 \\ \mathbb{0}_6 & \gamma_{6c}^p \end{pmatrix}, \quad (95)$$

$$\gamma_{6c}^x = \begin{pmatrix} 1.00601 & 0.00996299 & 0.110751 & 0.0220412 & 0.0996522 & 0.102581 \\ 0.00996299 & 1.1082 & 0.0996528 & 0.198639 & 1.0828 & 0.99682 \\ 0.110751 & 0.0996528 & 1.11751 & 0.224225 & 0.996235 & 1.12667 \\ 0.0220412 & 0.198639 & 0.224225 & 1.44671 & 1.98457 & 2.2454 \\ 0.0996522 & 1.0828 & 0.996235 & 1.98457 & 9.83666 & 9.97538 \\ 0.102581 & 0.99682 & 1.12667 & 2.2454 & 9.97538 & 10.2866 \end{pmatrix}, \quad (96)$$

$$\gamma_{6c}^p = \begin{pmatrix} 1.00601 & 0.00996299 & -0.110751 & -0.0220412 & -0.0996522 & 0.102581 \\ 0.00996299 & 1.1082 & -0.0996528 & -0.198639 & -1.0828 & 0.99682 \\ -0.110751 & -0.0996528 & 1.11751 & 0.224225 & 0.996235 & -1.12667 \\ -0.0220412 & -0.198639 & 0.224225 & 1.44671 & 1.98457 & -2.2454 \\ -0.0996522 & -1.0828 & 0.996235 & 1.98457 & 9.83666 & -9.97538 \\ 0.102581 & 0.99682 & -1.12667 & -2.2454 & -9.97538 & 10.2866 \end{pmatrix}. \quad (97)$$

Now, if we optimize numerically the difference (49) for the sum criterion (46) over the parameters  $\ell_{ij}^\alpha \in [-10, 10]$ , we arrive at  $D_S = -1.00$ . where

#### D.4.2 Tree 6d

For the tree 6d we guessed the witness matrix  $Z_{6d}$  as follows:

$$Z_{6d} = \frac{1}{2.7301} \begin{pmatrix} Z_{6d}^x & \mathbb{0}_6 \\ \mathbb{0}_6 & Z_{6d}^p \end{pmatrix}, \quad (98)$$

$$Z_{6d}^x = \begin{pmatrix} 1 & 0 & 0 & -0.1 & 0 & 0 \\ 0 & 1 & 0 & -0.1 & 0 & 0 \\ 0 & 0 & 1 & 0 & -0.1 & 0 \\ -0.1 & -0.1 & 0 & 0.27 & 0 & -0.05 \\ 0 & 0 & -0.1 & 0 & 0.02 & -0.01 \\ 0 & 0 & 0 & -0.05 & -0.01 & 0.0201 \end{pmatrix}$$

and

$$Z_{6d}^p = \begin{pmatrix} 1 & 0 & 0 & 0.1 & 0 & 0 \\ 0 & 0.25 & 0 & 0.05 & 0 & 0 \\ 0 & 0 & 1 & 0 & 0.1 & 0 \\ 0.1 & 0.05 & 0 & 0.27 & 0 & 0.05 \\ 0 & 0 & 0.1 & 0 & 0.02 & 0.01 \\ 0 & 0 & 0 & 0.05 & 0.01 & 0.0201 \end{pmatrix}.$$

In the next step, we find numerically the matrix  $S_{6d}$  symplectically diagonalizing  $Z_{6d}$ , which yields

$$\gamma_{6d} = S_{6d}^T S_{6d} = \begin{pmatrix} \gamma_{6d}^x & \mathbb{0}_6 \\ \mathbb{0}_6 & \gamma_{6d}^p \end{pmatrix}, \quad (99)$$

$$\gamma_{6d}^x = \begin{pmatrix} 1.01727 & 0.0150336 & 0.0200197 & 0.206136 & 0.200098 & 0.21641 \\ 0.0150336 & 0.513163 & 0.0200209 & 0.178237 & 0.200154 & 0.211026 \\ 0.0200197 & 0.0200209 & 1.10944 & 0.200099 & 1.09521 & 1.00374 \\ 0.206136 & 0.178237 & 0.200099 & 1.47744 & 1.99935 & 2.24369 \\ 0.200098 & 0.200154 & 1.09521 & 1.99935 & 9.96135 & 10.0452 \\ 0.21641 & 0.211026 & 1.00374 & 2.24369 & 10.0452 & 10.2858 \end{pmatrix}, \quad (100)$$

$$\gamma_{6d}^p = \begin{pmatrix} 1.01727 & 0.0300672 & 0.0200197 & -0.206136 & -0.200098 & 0.21641 \\ 0.0300672 & 2.05265 & 0.0400418 & -0.356474 & -0.400308 & 0.422052 \\ 0.0200197 & 0.0400418 & 1.10944 & -0.200099 & -1.09521 & 1.00374 \\ -0.206136 & -0.356474 & -0.200099 & 1.47744 & 1.99935 & -2.24369 \\ -0.200098 & -0.400308 & -1.09521 & 1.99935 & 9.96135 & -10.0452 \\ 0.21641 & 0.422052 & 1.00374 & -2.24369 & -10.0452 & 10.2858 \end{pmatrix}. \quad (101)$$

Now, if we optimize numerically the difference (49) for the sum criterion (46) over the parameters  $\ell_{ij}^\alpha \in$

$[-10, 10]$ , we arrive at  $D_S = -0.91$ .

where

#### D.4.3 Tree 6e

In the case of tree 6e we guessed the witness matrix  $Z_{6e}$  as

$$Z_{6e} = \frac{1}{3.1801} \begin{pmatrix} Z_{6e}^x & \mathbb{0}_6 \\ \mathbb{0}_6 & Z_{6e}^p \end{pmatrix}, \quad (102)$$

$$Z_{6e}^x = \begin{pmatrix} 1 & 0 & 0 & 0 & -0.1 & 0 \\ 0 & 1 & 0 & 0 & -0.1 & 0 \\ 0 & 0 & 0.01 & 0 & 0 & -0.01 \\ 0 & 0 & 0 & 0.01 & 0 & -0.01 \\ -0.1 & -0.1 & 0 & 0 & 0.03 & -0.01 \\ 0 & 0 & -0.01 & -0.01 & -0.01 & 0.0301 \end{pmatrix}$$

and

$$Z_{6e}^p = \begin{pmatrix} 4 & 0 & 0 & 0 & 0.2 & 0 \\ 0 & 1 & 0 & 0 & 0.1 & 0 \\ 0 & 0 & 1 & 0 & 0 & 0.1 \\ 0 & 0 & 0 & 1 & 0 & 0.1 \\ 0.2 & 0.1 & 0 & 0 & 0.03 & 0.01 \\ 0 & 0 & 0.1 & 0.1 & 0.01 & 0.0301 \end{pmatrix}.$$

From the numerically found symplectic matrix  $S_{6e}$  symplectically diagonalizing  $Z_{6e}$  we then construct the following CM:

$$\gamma_{6e} = S_{6e}^T S_{6e} = \begin{pmatrix} \gamma_{6e}^x & \mathbb{0}_6 \\ \mathbb{0}_6 & \gamma_{6e}^p \end{pmatrix}, \quad (103)$$

$$\gamma_{6e}^x = \begin{pmatrix} 2.07887 & 0.0788541 & 0.729928 & 0.729928 & 0.788929 & 0.749595 \\ 0.0788541 & 1.07884 & 0.730827 & 0.730827 & 0.788736 & 0.749621 \\ 0.729928 & 0.730827 & 19.0655 & 9.06554 & 7.28942 & 9.32218 \\ 0.729928 & 0.730827 & 9.06554 & 19.0655 & 7.28942 & 9.32218 \\ 0.788929 & 0.788736 & 7.28942 & 7.28942 & 6.89127 & 7.49556 \\ 0.749595 & 0.749621 & 9.32218 & 9.32218 & 7.49556 & 8.5861 \end{pmatrix}, \quad (104)$$

$$\gamma_{6e}^p = \begin{pmatrix} 0.519719 & 0.0394271 & -0.0364964 & -0.0364964 & -0.394465 & 0.374798 \\ 0.0394271 & 1.07884 & -0.0730827 & -0.0730827 & -0.788736 & 0.749621 \\ -0.0364964 & -0.0730827 & 0.190655 & 0.0906554 & 0.728942 & -0.932218 \\ -0.0364964 & -0.0730827 & 0.0906554 & 0.190655 & 0.728942 & -0.932218 \\ -0.394465 & -0.788736 & 0.728942 & 0.728942 & 6.89127 & -7.49556 \\ 0.374798 & 0.749621 & -0.932218 & -0.932218 & -7.49556 & 8.5861 \end{pmatrix}. \quad (105)$$

Now, if we optimize numerically the difference (49) for the sum criterion (46) over the parameters  $\ell_{ij}^\alpha \in [-10, 10]$ , we arrive at  $D_S = -0.65$ .

#### D.4.4 Tree 6f

In the case of the tree 6f we guess the six-mode witness matrix  $Z_{6f}$  to be

$$Z_{6f} = \frac{1}{75.4801} \begin{pmatrix} Z_{6f}^x & \mathbb{0}_6 \\ \mathbb{0}_6 & Z_{6f}^p \end{pmatrix}, \quad (106)$$

where

$$Z_{6f}^x = \begin{pmatrix} 25 & 0 & 0 & -0.5 & 0 & 0 \\ 0 & 25 & 0 & -0.5 & 0 & 0 \\ 0 & 0 & 25 & -0.5 & 0 & 0 \\ -0.5 & -0.5 & -0.5 & 0.04 & 0. & -0.01 \\ 0 & 0 & 0 & 0 & 25 & -0.5 \\ 0 & 0 & 0 & -0.01 & -0.5 & 0.0201 \end{pmatrix}$$

and

$$Z_{6f}^p = \begin{pmatrix} 25 & 0 & 0 & 5 & 0 & 0 \\ 0 & 25 & 0 & 0.5 & 0 & 0 \\ 0 & 0 & 25 & 0.5 & 0 & 0 \\ 5 & 0.5 & 0.5 & 2.02 & 0 & 0.1 \\ 0 & 0 & 0 & 0 & 0.01 & 0.01 \\ 0 & 0 & 0 & 0.1 & 0.01 & 0.0201 \end{pmatrix}.$$

From the symplectic matrix  $S_{6f}$  symplectically diagonalizing  $Z_{6f}$  we get the CM of the following form:

$$\gamma_{6f} = S_{6f}^T S_{6f} = \begin{pmatrix} \gamma_{6f}^x & \mathbb{0}_6 \\ \mathbb{0}_6 & \gamma_{6f}^p \end{pmatrix}, \quad (107)$$

$$\gamma_{6f}^x = \begin{pmatrix} 1.00888 & 0.0070959 & 0.0070959 & 0.44554 & 0.000907054 & 0.045205 \\ 0.0070959 & 1.00531 & 0.00530564 & 0.265838 & 0.00090708 & 0.0452774 \\ 0.0070959 & 0.00530564 & 1.00531 & 0.265838 & 0.00090708 & 0.0452774 \\ 0.44554 & 0.265838 & 0.265838 & 12.3541 & 0.0453557 & 2.26827 \\ 0.000907054 & 0.00090708 & 0.00090708 & 0.0453557 & 0.020908 & 0.0454074 \\ 0.045205 & 0.0452774 & 0.0452774 & 2.26827 & 0.0454074 & 1.27089 \end{pmatrix}, \quad (108)$$

$$\gamma_{6f}^p = \begin{pmatrix} 1.00889 & 0.00267199 & 0.00267199 & -0.0446333 & -0.0453539 & 0.0452056 \\ 0.00267199 & 1.00044 & 0.000437932 & -0.0224336 & -0.00453415 & 0.00444848 \\ 0.00267199 & 0.000437932 & 1.00044 & -0.0224336 & -0.00453415 & 0.00444848 \\ -0.0446333 & -0.0224336 & -0.0224336 & 0.124334 & 0.226785 & -0.226828 \\ -0.0453539 & -0.00453415 & -0.00453415 & 0.226785 & 52.2702 & -2.27039 \\ 0.0452056 & 0.00444848 & 0.00444848 & -0.226828 & -2.27039 & 1.27089 \end{pmatrix}. \quad (109)$$

Now, if we optimize numerically the difference (49) for the sum criterion (46) over the parameters  $\ell_{ij}^\alpha \in [-10, 10]$ , we arrive at  $D_S = -0.13$ .

## E Numerical example of robust GME state

This section contains CM of state found by Gaussian analog [43] of the iterative algorithm [41], as is done in Sec. 5.1.2. In contrast to the states with CMs  $\gamma_1$  and  $\gamma_2$  presented there, we used additional constraint restricting the amount of squeezing needed to prepare the state with given CM to maximally  $-5$  dB. The

where

state with CM

$$\gamma_7 = \begin{pmatrix} 3.96432 & 3.33486 & 1.66686 \\ 3.33486 & 3.60552 & 1.84641 \\ 1.66686 & 1.84641 & 1.27596 \end{pmatrix} \oplus \begin{pmatrix} 3.48332 & -2.61754 & 3.45572 \\ -2.61754 & 3.13354 & -3.379668 \\ 3.45572 & -3.79668 & 7.73756 \end{pmatrix} \quad (110)$$

is detected as GME by criterion (53) with the difference  $D_P = -0.111$  over the parameters  $\ell_{ij}^\alpha \in [-1, 1]$  given in Tab. 11.

## References

- [1] Reinhard F. Werner. “Quantum states with Einstein-Podolsky-Rosen correlations admitting a hidden-variable model”. *Phys. Rev. A* **40**, 4277–4281 (1989).

Table 11: Rounded values of the parameters  $\ell_{ij}^\alpha \in [-1, 1]$ ,  $\alpha = x, p$ , used to calculate the difference (48) for the product criterion (53) and the CM  $\gamma_7$ , Eq. (110).

$\ell_{11}^x$	0.67
$\ell_{12}^x$	-0.76
$\ell_{22}^x$	0.68
$\ell_{23}^x$	-1.00
$\ell_{33}^x$	0.01
$\ell_{11}^p$	0.82
$\ell_{12}^p$	1.00
$\ell_{22}^p$	1.00
$\ell_{23}^p$	0.61
$\ell_{33}^p$	0.01

- [2] Ryszard Horodecki, Paweł Horodecki, Michał Horodecki, and Karol Horodecki. “Quantum entanglement”. *Rev. Mod. Phys.* **81**, 865–942 (2009).
- [3] Howard M. Wiseman, Steven J. Jones, and Andrew C. Doherty. “Steering, entanglement, non-locality, and the Einstein-Podolsky-Rosen paradox”. *Phys. Rev. Lett.* **98**, 140402 (2007).
- [4] Roope Uola, Ana C. S. Costa, H. Chau Nguyen, and Otfried Gühne. “Quantum steering”. *Rev. Mod. Phys.* **92**, 015001 (2020).
- [5] John S. Bell. “On the Einstein Podolsky Rosen paradox”. *Phys. Phys. Fiz.* **1**, 195–200 (1964).
- [6] Nicolas Brunner, Daniel Cavalcanti, Stefano Pironio, Valerio Scarani, and Stephanie Wehner. “Bell nonlocality”. *Rev. Mod. Phys.* **86**, 419–478 (2014).
- [7] Michael N. Nielsen and Isaac L. Chuang. “Quantum computation and quantum information”. Cambridge University Press. (2000).
- [8] Jean-Daniel Bancal, Nicolas Gisin, Yeong-Cherng Liang, and Stefano Pironio. “Device-independent witnesses of genuine multipartite entanglement”. *Phys. Rev. Lett.* **106**, 250404 (2011).
- [9] Daniel M. Greenberger, Michael A. Horne, and Anton Zeilinger. “Bell’s Theorem, Quantum Theory, and Conceptions of the Universe”. Page 69. Kluwer, Dordrecht. (1989).
- [10] Jian-Wei Pan, Dik Bouwmeester, Matthew Daniell, Harald Weinfurter, and Anton Zeilinger. “Experimental test of quantum nonlocality in three-photon Greenberger–Horne–Zeilinger entanglement”. *Nature* **403** (2000).
- [11] Thomas Monz, Philipp Schindler, Julio T. Barreiro, Michael Chwalla, Daniel Nigg, William A. Coish, Maximilian Harlander, Wolfgang Hänsel, Markus Hennrich, and Rainer Blatt. “14-qubit entanglement: Creation and coherence”. *Phys. Rev. Lett.* **106**, 130506 (2011).
- [12] Mark Hillery, Vladimír Bužek, and André Berthiaume. “Quantum secret sharing”. *Phys. Rev. A* **59**, 1829–1834 (1999).
- [13] Anders Karlsson and Mohamed Bourennane. “Quantum teleportation using three-particle entanglement”. *Phys. Rev. A* **58**, 4394–4400 (1998).
- [14] Hidehiro Yonezawa, Takao Aoki, and Akira Furusawa. “Demonstration of a quantum telepor-

tation network for continuous variables”. *Nature* **431** (2004).

- [15] Vittorio Giovannetti, Seth Lloyd, and Lorenzo Maccone. “Quantum-enhanced measurements: Beating the standard quantum limit”. *Science* **306**, 1330–1336 (2004).
- [16] Géza Tóth. “Multipartite entanglement and high-precision metrology”. *Phys. Rev. A* **85**, 022322 (2012).
- [17] Robert Raussendorf and Hans J. Briegel. “A one-way quantum computer”. *Phys. Rev. Lett.* **86**, 5188–5191 (2001).
- [18] Philip Walther, Kevin J. Resch, Terry Rudolph, Emmanuel Schenck, Harald Weinfurter, Vlatko Vedral, Markus Aspelmeyer, and Anton Zeilinger. “Experimental one-way quantum computing”. *Nature* **434**, 169–176 (2005).
- [19] Michael Epping, Hermann Kampermann, Chiara Macchiavello, and Dagmar Bruß. “Multi-partite entanglement can speed up quantum key distribution in networks”. *New J. Phys.* **19**, 093012 (2017).
- [20] Jérémie Ribeiro, Gláucia Murtas, and Stephanie Wehner. “Fully device-independent conference key agreement”. *Phys. Rev. A* **97**, 022307 (2018).
- [21] Nicolai Friis, Oliver Marty, Christine Maier, Cornelius Hempel, Milan Holzapfel, Petar Jurcevic, Martin B. Plenio, Marcus Huber, Christian Roos, Rainer Blatt, and Ben Lanyon. “Observation of entangled states of a fully controlled 20-qubit system”. *Phys. Rev. X* **8**, 021012 (2018).
- [22] Ming Gong, Ming-Cheng Chen, Yarui Zheng, Shiyu Wang, Chen Zha, Hui Deng, Zhiguang Yan, Hao Rong, Yulin Wu, Shaowei Li, Fusheng Chen, Youwei Zhao, Futian Liang, Jin Lin, Yu Xu, Cheng Guo, Lihua Sun, Juno Clark, Hao-hua Wang, Chengzhi Peng, Chao-Yang Lu, Xiaobo Zhu, and Jian-Wei Pan. “Genuine 12-qubit entanglement on a superconducting quantum processor”. *Phys. Rev. Lett.* **122**, 110501 (2019).
- [23] Xi-Lin Wang, Yi-Han Luo, He-Liang Huang, Ming-Cheng Chen, Zu-En Su, Chang Liu, Chao Chen, Wei Li, Yu-Qiang Fang, Xiao Jiang, Jun Zhang, Li Li, Nai-Le Liu, Chao-Yang Lu, and Jian-Wei Pan. “18-qubit entanglement with six photons’ three degrees of freedom”. *Phys. Rev. Lett.* **120**, 260502 (2018).
- [24] Sirui Cao, Bujiao Wu, Fusheng Chen, Ming Gong, Yulin Wu, Yangsen Ye, Chen Zha, Haoran Qian, Chong Ying, Shaojun Guo, et al. “Generation of genuine entanglement up to 51 superconducting qubits”. *Nature* **619**, 738–742 (2023).
- [25] Christian Weedbrook, Stefano Pirandola, Raúl García-Patrón, Nicolas J. Cerf, Timothy C. Ralph, Jeffrey H. Shapiro, and Seth Lloyd. “Gaussian quantum information”. *Rev. Mod. Phys.* **84**, 621–669 (2012).
- [26] Lynden K. Shalm, Deny R. Hamel, Zhizhong

- Yan, Christoph Simon, Kevin J. Resch, and Thomas Jennewein. “Three-photon energy–time entanglement”. *Nat. Phys.* **9**, 19–22 (2013).
- [27] Seiji Armstrong, Meng Wang, Run Yan Teh, Qihuang Gong, Qiongyi He, Jiri Janousek, Hans-Albert Bachor, Margaret D Reid, and Ping Koy Lam. “Multipartite Einstein–Podolsky–Rosen steering and genuine tripartite entanglement with optical networks”. *Nat. Phys.* **11**, 167–172 (2015).
- [28] Stefan Gerke, Jan Sperling, Werner Vogel, Yin Cai, Jonathan Roslund, Nicolas Treps, and Claude Fabre. “Full multipartite entanglement of frequency-comb Gaussian states”. *Phys. Rev. Lett.* **114**, 050501 (2015).
- [29] Evgeny Shchukin and Peter van Loock. “Generalized conditions for genuine multipartite continuous-variable entanglement”. *Phys. Rev. A* **92**, 042328 (2015).
- [30] Moran Chen, Nicolas C. Menicucci, and Olivier Pfister. “Experimental realization of multipartite entanglement of 60 modes of a quantum optical frequency comb”. *Phys. Rev. Lett.* **112**, 120505 (2014).
- [31] Shota Yokoyama, Ryuji Ukai, Seiji C. Armstrong, Chanond Sornphiphatphong, Toshiyuki Kaji, Shigenari Suzuki, Jun-ichi Yoshikawa, Hidehiro Yonezawa, Nicolas C. Menicucci, and Akira Furusawa. “Ultra-large-scale continuous-variable cluster states multiplexed in the time domain”. *Nat. Photonics* **7**, 982–986 (2013).
- [32] Jun-ichi Yoshikawa, Shota Yokoyama, Toshiyuki Kaji, Chanond Sornphiphatphong, Yu Shiozawa, Kenzo Makino, and Akira Furusawa. “Invited article: Generation of one-million-mode continuous-variable cluster state by unlimited time-domain multiplexing”. *APL Photonics* **1** (2016).
- [33] Philipp Hyllus and Jens Eisert. “Optimal entanglement witnesses for continuous-variable systems”. *New J. Phys.* **8**, 51 (2006).
- [34] Mauro Paternostro, David Vitali, Sylvain Gigan, M. S. Kim, Caslav Brukner, Jens Eisert, and Markus Aspelmeyer. “Creating and probing multipartite macroscopic entanglement with light”. *Phys. Rev. Lett.* **99**, 250401 (2007).
- [35] Shan W. Jolin, Gustav Andersson, J. C. Rivera Hernández, Ingrid Strandberg, Fernando Quijandría, José Aumentado, Riccardo Borgani, Mats O. Tholén, and David B. Haviland. “Multipartite entanglement in a microwave frequency comb”. *Phys. Rev. Lett.* **130**, 120601 (2023).
- [36] Run Y. Teh and Margaret D. Reid. “Criteria for genuine  $N$ -partite continuous-variable entanglement and Einstein–Podolsky–Rosen steering”. *Phys. Rev. A* **90**, 062337 (2014).
- [37] Fabricio Toscano, A. Saboia, Ardiley T. Avelar, and Stephen P. Walborn. “Systematic construction of genuine-multipartite-entanglement criteria in continuous-variable systems using uncertainty relations”. *Phys. Rev. A* **92**, 052316 (2015).
- [38] Peter van Loock and Akira Furusawa. “Detecting genuine multipartite continuous-variable entanglement”. *Phys. Rev. A* **67**, 052315 (2003).
- [39] Lu-Ming Duan, Géza Giedke, J. Ignacio Cirac, and Peter Zoller. “Inseparability criterion for continuous variable systems”. *Phys. Rev. Lett.* **84**, 2722–2725 (2000).
- [40] Vittorio Giovannetti, Stefano Mancini, David Vitali, and Paolo Tombesi. “Characterizing the entanglement of bipartite quantum systems”. *Phys. Rev. A* **67**, 022320 (2003).
- [41] Marius Paraschiv, Nikolai Miklin, Tobias Mroder, and Otfried Gühne. “Proving genuine multiparticle entanglement from separable nearest-neighbor marginals”. *Phys. Rev. A* **98**, 062102 (2018).
- [42] Michal Mičuda, Robert Stárek, Jan Provaník, Olga Leskovjanová, and Ladislav Mišta Jr. “Verifying genuine multipartite entanglement of the whole from its separable parts”. *Optica* **6**, 896–901 (2019).
- [43] Viktor Nordgren, Olga Leskovjanová, Jan Provaník, Adam Johnston, Natalia Korolkova, and Ladislav Mišta. “Certifying emergent genuine multipartite entanglement with a partially blind witness”. *Phys. Rev. A* **106**, 062410 (2022).
- [44] Oleg Gittsovich, Philipp Hyllus, and Otfried Gühne. “Multiparticle covariance matrices and the impossibility of detecting graph-state entanglement with two-particle correlations”. *Phys. Rev. A* **82**, 032306 (2010).
- [45] Atsushi Higuchi, Anthony Sudbery, and Jason Szulc. “One-qubit reduced states of a pure many-qubit state: Polygon inequalities”. *Phys. Rev. Lett.* **90**, 107902 (2003).
- [46] Sergey Bravyi. “Requirements for compatibility between local and multipartite quantum states” (2003). [arXiv:quant-ph/0301014](https://arxiv.org/abs/quant-ph/0301014).
- [47] Lars Erik Würflinger, Jean-Daniel Bancal, Antonio Acín, Nicolas Gisin, and Tamás Vértesi. “Nonlocal multipartite correlations from local marginal probabilities”. *Phys. Rev. A* **86**, 032117 (2012).
- [48] Wolfgang Dür, J. Ignacio Cirac, and Rolf Tarrach. “Separability and distillability of multipartite quantum systems”. *Phys. Rev. Lett.* **83**, 3562–3565 (1999).
- [49] Géza Giedke, Barbara Kraus, Maciej Lewenstein, and J. Ignacio Cirac. “Separability properties of three-mode gaussian states”. *Phys. Rev. A* **64**, 052303 (2001).
- [50] Marco Piani and Caterina E. Mora. “Class of positive-partial-transpose bound entangled

- states associated with almost any set of pure entangled states”. *Phys. Rev. A* **75**, 012305 (2007).
- [51] Otfried Gühne and Géza Tóth. “Entanglement detection”. *Phys. Rep.* **474**, 1–75 (2009).
- [52] Michał Horodecki, Paweł Horodecki, and Ryszard Horodecki. “Separability of mixed states: necessary and sufficient conditions”. *Phys. Lett. A* **223**, 1–8 (1996).
- [53] Barbara M. Terhal. “Bell inequalities and the separability criterion”. *Phys. Lett. A* **271**, 319–326 (2000).
- [54] Rajiah Simon. “Peres-Horodecki separability criterion for continuous variable systems”. *Phys. Rev. Lett.* **84**, 2726–2729 (2000).
- [55] Peter van Loock and Samuel L. Braunstein. “Multipartite entanglement for continuous variables: A quantum teleportation network”. *Phys. Rev. Lett.* **84**, 3482–3485 (2000).
- [56] Janet Anders. “Estimating the degree of entanglement of unknown Gaussian states” (2006). [arXiv:quant-ph/0610263](https://arxiv.org/abs/quant-ph/0610263).
- [57] Douglas Brent West et al. “Introduction to graph theory”. Volume 2. Prentice hall Upper Saddle River. (2001).
- [58] Peter Steinbach. “Field guide to simple graphs”. Volume 3. Design Lab, Albuquerque. (1999).
- [59] Richard Otter. “The number of trees”. *Ann. Math.* **49**, 583–599 (1948).
- [60] “The on-line encyclopedia of integer sequences”. url: [oeis.org](https://oeis.org). Sequence A000055.
- [61] Paul R. Halmos. “Finite dimensional vector spaces”. Annals of Mathematics Studies. Princeton University Press. (1948).
- [62] Roger A. Horn and Charles R. Johnson. “Matrix analysis”. Cambridge university press. (1985).
- [63] Gene H. Golub and Charles F. Van Loan. “Matrix computations”. Johns Hopkins Studies in the Mathematical Sciences. Johns Hopkins University Press. (2013). 3 edition.
- [64] Jack J. Dongarra, James R. Bunch, Cleve B. Moler, and G. W. Stewart. “LINPACK Users’ Guide”. Other Titles in Applied Mathematics. Society for Industrial and Applied Mathematics. (1979).
- [65] S. Mitchell Hedetniemi, E. J. Cockayne, and S. T. Hedetniemi. “Linear algorithms for finding the Jordan center and path center of a tree”. *Transp. Sci.* **15**, 98–114 (1981).
- [66] Holger F. Hofmann and Shigeki Takeuchi. “Violation of local uncertainty relations as a signature of entanglement”. *Phys. Rev. A* **68**, 032103 (2003).
- [67] Wolfram Research, Inc. “Mathematica, Version 12.3”. Champaign, IL, 2021.
- [68] Run Yan Teh, Manuel Gessner, Margaret D. Reid, and Matteo Fadel. “Full multipartite steering inseparability, genuine multipartite steering, and monogamy for continuous-variable systems”. *Phys. Rev. A* **105**, 012202 (2022).
- [69] John Williamson. “On the algebraic problem concerning the normal forms of linear dynamical systems”. *Am. J. Math.* **58**, 141–163 (1936).
- [70] Evgeny Shchukin and Peter van Loock. “Tripartite separability conditions exponentially violated by Gaussian states”. *Phys. Rev. A* **90**, 012334 (2014).
- [71] Da Zhang, David Barral, Yanpeng Zhang, Min Xiao, and Kamel Bencheikh. “Genuine tripartite non-Gaussian entanglement”. *Phys. Rev. Lett.* **130**, 093602 (2023).
- [72] Qiongyi Y. He and Margaret D. Reid. “Genuine multipartite Einstein-Podolsky-Rosen steering”. *Phys. Rev. Lett.* **111**, 250403 (2013).
- [73] Jaromír Fiurášek and Ladislav Mišta. “Gaussian localizable entanglement”. *Phys. Rev. A* **75**, 060302 (2007).
- [74] Guifre Vidal and Reinhard F. Werner. “Computable measure of entanglement”. *Phys. Rev. A* **65**, 032314 (2002).
- [75] Jason L. Pereira, Leonardo Banchi, and Stefano Pirandola. “Symplectic decomposition from submatrix determinants”. *Proc. R. Soc. A* **477**, 20210513 (2021).